

Extending the lifetime of NB-IoT devices through Energy-Harvesting techniques

Anand Haridas

EWI

EXTENDING THE LIFETIME OF NB-IoT DEVICES THROUGH ENERGY-HARVESTING TECHNIQUES

by

Anand Haridas

in partial fulfillment of the requirements for the degree of

Master of Science

in Embedded systems

at the Delft University of Technology,

to be defended publicly on November 7th, 2018

Supervisor : Dr. R. Venkatesha Prasad
Daily Supervisor : Dr. ir. Vijay S. Rao
Thesis committee : Dr. ir. Fernando Kuipers, TU Delft
Dr. ir. Mathijs De Weerd, TU Delft

An electronic version of this thesis is available at <http://repository.tudelft.nl/>.

ABSTRACT

For the Internet of Things (IoT) applications that send a few bytes of sensor information infrequently, several long-range IoT technologies have been conceived. Narrowband IoT (NB-IoT) is one of them that stands out due to its extended coverage, high penetrability, and high reliability features. Envisaged long device lifetime and the extended coverage are important aspects of the NB-IoT radio technology that has garnered attention. With the increase in applications to connect a large number of devices over long distances, it becomes crucial for the technology to meet the lifetime expectations set in the standards. However, the empirical lifetime estimations, done as part of this work, indicate that the current devices do not meet the lifetime estimates targeted in the 3GPP standards, lasting for 2.38 years when exchanging 200 bytes of data at a rate of 1 message per day. Potential solutions include energy-harvesting to augment the battery lifetime. However, due to the spatiotemporal variation in the amount of energy harvested, the supplemented energy levels will be less than the energy consumption. Therefore, it becomes essential for the sensor device enabled with NB-IoT communication technology to implement energy management techniques to maximize the utility to the application it serves based on its energy situation. Further, the coverage enhancement techniques inbuilt in the technology forms a major contributor to the low device lifetime. With the NB-IoT radio block considered as a 'black box' with no access to the software stack, innovative solutions are required to reduce the energy consumption of sending payloads without losing out on coverage.

To this end, this work proposes a framework called xTEND to increase the utility of the device while being energy-efficient in deep coverage scenarios. In xTEND, the decision to transmit a payload is done by modeling the problem as a 0/1 incremental knapsack problem. A threshold policy is proposed that optimally schedules payloads in a given finite horizon, with a low complexity method to compute it on the device. Furthermore, as the coverage enhancement techniques deplete the battery soon for deep coverage scenarios, we propose to increase the transmission power adaptively based on the channel conditions. The framework is evaluated with an existing scheme in the literature that performs energy management and is shown to outperform in different traffic distributions. Further, with the framework, an average 3.8 J of energy savings and 8.027 s of time savings is obtained in the shared and control channels of the physical layer. This results in an average lifetime extension of 20 % in deep coverage scenarios. With the only requirement of access to the power amplifier embedded on the NB-IoT chipset, the framework can be implemented on the deployed sensor device.

PREFACE

The last nine months have been an incredible uphill journey in my academic life, both in learning and in efforts invested. Amongst all the frustrations and sleepless nights, in retrospect, I feel the journey has been kind to me. The entire experience has proved to be educational and challenging, which is exactly what I was looking for when I began my work nine months back.

There are a number of people I would like to thank for the successful completion of the thesis. On the top of the list is my supervisor, VP. I would like to thank him for providing me with such a wonderful opportunity. All the discussions and pointers have definitely proved to be helpful. I would like to thank Sujay Narayana for his support in setting up the required hardware and his guidance through my experiments. My friend Kiran Kumar was kind enough to accommodate my experiments in his room and for this I am grateful. Further, I would like to thank Nikos Kouvelas, Weizheng Wang (Eric), Venkat Balasubramiam, Kishore Chandra for all the coffees and the discussions over the coffees. The coffee breaks helped dissolve the stress and were quite informative.

The person I could not thank enough is my daily supervisor, Vijay S. Rao. He kindly provided a patient ear to all my queries and was up for innumerable discussions to make the work better. I would like to thank him for being a mentor.

My strongest support system in Delft have been the people who have made Delft far closer to home. For this, I would like to thank Jesil J. Kurian, Nitin P. Prasad, Akhil Krishnakumar, Rahul Ravindran, Chetan Srivatsa and Sanjay Ganeshan.

I would like to thank George, Amrutha, Array, Aditya, and Ashwin, for being there irrespective of anything. Finally, I would like to thank my fallback system for eternity - my mother, father, and brother. All their hard work and efforts are reflected in the fruition of this work.

*Anand Haridas
Delft, October 2018*

CONTENTS

Abstract	v
List of Figures	ix
List of Tables	xi
1 Introduction	1
1.1 Problem statement and Motivation	2
1.2 Methodology	4
1.3 Contributions	5
1.4 Organization	5
2 Background & Related Work	7
2.1 Physical layer: a short overview	7
2.1.1 A frame level perspective.	7
2.1.2 Physical channels, physical signals, and scheduling in time-frequency frame	9
2.2 Physical transactions in NB-IoT.	11
2.2.1 Attach Procedure: When the device powers up.	11
2.2.2 Solutions in the standards to reduce energy consumption	12
2.2.3 Payload exchange procedure.	12
2.3 Related work	13
3 Energy Characterization and EH Feasibility study	17
3.1 Energy characterization.	17
3.1.1 Energy measurements	17
3.1.2 Energy consumption model	19
3.1.3 Lifetime estimation	22

3.2	Ambient energy to the rescue	23
3.2.1	Energy-harvesting profiles	23
3.2.2	Converting energy into packets	24
3.3	Challenges	25
3.3.1	Challenges in energy-harvesting	25
3.3.2	Challenges in NB-IoT	26
3.4	Summary	27
4	Energy extension Framework	29
4.1	Motivation	29
4.2	Design goals	30
4.3	Overview of the xTEND Framework	30
4.4	The EVAPS Module	30
4.5	The Channel-Aware Radio Module	37
4.6	Summary	40
5	Performance Evaluation	41
5.1	Smart parking use-case	41
5.2	System evaluation.	41
5.2.1	Evaluation Scenario	42
5.2.2	EVAPS evaluation	43
5.2.3	ChAR evaluation	47
5.3	Summary	49
6	Conclusions and Future Work	51
6.1	Conclusions.	51
6.2	Future Work.	52
	Bibliography	57

LIST OF FIGURES

1.1	Evolution of the LPWAN technologies [1]	2
1.2	Block diagram of the xTEND framework in a UE	4
2.1	the different deployment modes [2] of NB-IoT	7
2.2	Frame-level structure [3] representing the slot, subframe, frame and hyperframe	8
2.3	Scheduling of transport blocks in the uplink and downlink	10
2.4	A payload exchange procedure between the UE and the base station	11
2.5	PSM and eDRX procedures. The eDRX cycle can extend up to 175 min. [4]	13
3.1	The experimental setup	18
3.2	Map indicating locations in the city of Delft where the measurements were taken	18
3.3	Energy consumption measurements for different payload sizes for 4 different coverage conditions	19
3.4	The current trace for a payload exchange obtained using the power monitor. The transmission, reception and idle mode stages are presented seperately in row 2.	20
3.5	Lifetime estimations of the UE based on empirical measurements when compared to the expected measurements [3]	22
3.6	Window Sill - Averaged energy reading over 378 days for each 1 h period	24
3.7	Book Shelf - Averaged energy reading over 341 days for each 1 h period	24
3.8	Outdoors - Averaged energy reading over 365 days for each 1 h period	25
3.9	The gain represented in terms of additional packets that can be send	26
4.1	Payloads in periodic (row 1) and event-triggered applications (row 2)	32
4.2	The formation of the table structure as part of the dynamic programming solution to solve the incremental knapsack problem	35
4.3	Representation of the lookup table with four payloads and their capacity thresholds	35
4.4	Screenshot of the DCI message log analyzed on the Accuver XCAL tool. The repetition numbers are highlighted.	38

4.5	The Repetition count for NPUSCH (UL RN), NPDSCH(DL RN), and NPDCCH (DCI RN) subframes of a 200 bytes payload in both uplink and downlink, with (left bars) and without (right bars) the additional gain	39
4.6	The block diagram to implement ChAR block to NB-Iot radio modem for analysis.	39
5.1	Periodic application serving 4 payloads of the same type. Additional value accumulated with respect to no framework scenario (left), the total number of payloads scheduled (center) and the capacity left at the end of the evaluation period (right) with varying finite horizon and evaluation periods for the schemes considered	43
5.2	Periodic application serving 12 payloads of the same type. Additional value accumulated with respect to no framework scenario (left), the total number of payloads scheduled (center) and the capacity left at the end of the evaluation period (right) with varying finite horizon and evaluation periods for the schemes considered.	43
5.3	Periodic application serving 4 payloads of different type. Additional value accumulated with respect to no framework scenario (left), the total number of payloads scheduled (center) and the capacity left at the end of the evaluation period (right) with varying finite horizon and evaluation periods for the schemes considered.	44
5.4	Periodic application serving 12 payloads of different type. Additional value accumulated with respect to no framework scenario (left), the total number of payloads scheduled (center) and the capacity left at the end of the evaluation period (right) with varying finite horizon and evaluation periods for the schemes considered.	44
5.5	Only events scenario: ratios of values accumulated, number of payloads scheduled by the clairvoyant algorithm to that of EVAPS ver. 1, EVAPSA ver. 2 and Jumping threshold. The functions val() and count() returns the total value accumulated and the number of payloads scheduled.	45
5.6	Periodic+events scenario: ratios of values accumulated, number of payloads scheduled by the clairvoyant algorithm to that of EVAPS ver. 1, EVAPSA ver. 2 and Jumping threshold. The functions val() and count() returns the total value accumulated and the number of payloads scheduled.	47
5.7	Experimental setup for ChAR evaluation	47
5.8	Energy savings with additional gain due to reduced coverage enhancement affects	48
5.9	Time savings with additional gain due to reduced coverage enhancement affects	48

LIST OF TABLES

3.1	The different components in the active mode of an message transaction	20
5.1	Average time savings for each physical channel	49

1

INTRODUCTION

The Internet, over the last few decades, has had a global impact on the ability of humans to exchange information. More physical devices embedded with the ability to connect to and exchange data over the internet are built every single day. The rise of this capability in appliances forms the backbone for applications that rely on data collected by sensor devices, deployed far away from services that require them. This concept of connected devices or the ‘Internet of Things’ (IoT) paves way for Machine to Machine (M2M) and Machine to Person communications [5]. Currently, an estimate of 6.4 billion IoT devices exists (without accounting for smartphones and laptops), with a projection that this number will double in five years time [6]. With more IoT devices, organizations such as the 3rd Generation Partnership Project (or 3GPP), comprising of multiple standard development bodies that provide specifications for different telecommunication technologies, has increased the emphasis for M2M communications.

The M2M communication or Machine Type communication (MTC) (as specified by 3GPP) has a broad set of use cases. These use cases can be characterized by the size of data exchanges, the rate of exchange, delay tolerance, magnitude of devices involved etc. Further, they can be classified on the basis of technology used to realize them. A significant portion of the existing market for IoT is facilitated by the short radio technologies that are implemented on the unlicensed spectrum [5] such as Wi-Fi, Zigbee etc. Further, applications such as smart meters, logistics tracking etc. demand wide area networks with a massive number of devices connected via a long-range radio technology. Typically such applications are characterized by small and infrequent data exchanges coupled with relaxed delay constraints, with the sensor devices deployed in areas devoid of wired power. Solutions to such networks in both licensed and unlicensed spectrum, termed as Low Power Wide Area Networks (LPWAN), have existed for almost a decade [7] are shown in Figure 1.1. Technological solutions in the unlicensed spectrum include proprietary radio technologies such as Sigfox and LoRa, designed specifically for MTC. The advent of these technologies challenged existing solutions that were based on the mature Global System for Communication (GSM) / General Packet Radio Service (GPRS). But these solutions come with their own hardware and software needs.

Traditionally, 3GPP technologies have focused on providing quality voice and data services. Utilization of existing systems to facilitate data transactions for IoT would result in network overload due to the required amount of signaling overheads for obtaining and setting up of radio resources [2], the high cost of the massive number of devices and requirements of coverage and availability of base sta-



Figure 1.1: Evolution of the LPWAN technologies [1]

tions [7]. Owing to the growing demands and the need to secure the market, the 3GPP organization has specified new technologies in the later standards. Although they are derivatives of existing radio technologies such as LTE, they are optimized to perform the required functions. These technologies are enhanced Machine Type Communication (eMTC), LTE-M, and Narrowband-IoT (NB-IoT). Among the new technologies, the key differences lie in radio frequency bandwidth utilization, indoor coverage support, and deployment modes. Narrowband IoT or NB-IoT stands out with the least bandwidth utilization and the lowest throughput, further reducing the costs involved in terms of energy, money, and complexity. In this work, the energy consumption and lifetime of devices deployed to make use of NB-IoT technology is of concern. The following sections in the chapter present the problem statement, the motivation, and the contributions of the thesis.

1.1. PROBLEM STATEMENT AND MOTIVATION

Narrowband-Internet of Things (NB-IoT) is one of the Low-Power Wide Area Networks (LPWANs) technologies that has been standardized by the third-generation partnership project (3GPP) working group [8]. Similar to the other LPWAN technologies, such as LoRaWAN and SigFox [9], the sensor devices in NB-IoT (also called User Equipment or UEs) transmit data directly to a gateway or base-station (also called e-Node-B or eNB). The number of nodes using NB-IoT for various applications is expected to rise rapidly as it is backed by cellular operators, such as T-Mobile and Vodafone [10], who provide guarantees on their offered services.

The applications or use-cases supported by NB-IoT are smart parking, smart garbage bins to logistics and pet tracking [7]. The application characteristics are that these UEs send small amounts of data over large intervals of time and sometimes with relaxed latency requirements for massive IoT applications [11]. As with the other LPWAN technologies, NB-IoT has to be a low-power and scalable technology. NB-IoT envisions that a UE will last for 10+ years and can connect up to 67,000 devices/km². Furthermore, NB-IoT can connect devices that are placed in deep indoor regions (for instance, a cellular parking area that is 6 levels below the ground) where other LPWANs typically fail [12]. This is achieved by coverage enhancement techniques including modulation and coding rate (MCS), repetitions of a subframe, and higher transmission power (up to +23 dBm).

The UEs are typically battery-powered due to the flexibility offered in deployment and portability for mobile applications. As is typical of 3GPP standards, each time a packet has to be sent, a request has to be made to the base station or eNodeB (eNB). Only after the request is accepted and radio resources

are allocated, the data packet is sent. These signaling overheads cause stress on the battery, especially in deep coverage scenarios. In order to reduce the energy consumption, the NB-IoT standard specifies techniques such as Power Saving Mode (PSM) and extended Discontinuous Reception (eDRX) modes [8] that enable duty-cycling of the radio. However, even with these modes, the devices will not last as long as expected [13] in a practical deployment, especially in deep coverage scenarios due to the timer configurations, the rate of message exchange and coverage enhancement techniques.

This work is done in collaboration with a network operator who has recently deployed NB-IoT in the Netherlands. The measurements for power consumption and lifetime estimations are performed using the evaluation board from U-Blox (EVKN2) which holds the Sara N211 radio modem [14]. The power measurements are obtained using the power monitor from Monsoon solutions [15]. The network was profiled for power consumption at various locations in our city encompassing various coverage scenarios. Based on these measurements lifetime estimations were drawn and it was observed that the UE does not meet the expectations set by the standards in all the cases. For instance, the theoretical estimation of the lifetime for a UE in deep coverage sending 200 bytes packet per day was 11.3 years with a 5 Wh battery [3]; our measurements indicate the device can last slightly more than 2.3 years.

As NB-IoT is an extension to the 4G LTE standard, the NB-IoT UE is a “black box”, i.e., the UE cannot be tweaked. All of the intelligence resides in the eNB, and the UE acts only based on the commands from eNB. For instance, the UE can request for switching to PSM (Power Saving Mode), which must be acknowledged or overridden by the eNB. Although the energy consumption of the device is mostly due to the communications, no change can be made in the networking stack or even adapt duty-cycle independently. Furthermore, the intelligence on the eNB was not allowed to be changed as the operator has no access to the source code except tuning a few parameters. This mandates the need to design innovative solutions.

Among the primary goals set for the standard, low device lifetime is crucial to the technology. Based on the lifetime estimations made on empirical energy measurements of message exchanges with the base station with the aforementioned limitations, this work strives to achieve the following research objective:

To extend the time to depletion of an NB-IoT device battery using energy-harvesting techniques such that the utility of the device for the application is maximized and the effects of the coverage enhancement techniques on the device lifetime is countered.

The aforementioned research objective is coupled with the following research challenges:

- The amount of energy harvested in one hour, especially in indoors, is typically far lower than sending one message on NB-IoT.
- The spatiotemporal dependency of harvested energy implies variations in the amount of incoming energy for different applications. The solution must maximize the utility of the device for the application in all such scenarios.
- The solution must deal with messages of different packet size and priorities, employed in different traffic distributions, so as to maximize the utility of the application based on the capacity available at an instant.
- The solution must minimize the effects of the coverage enhancement techniques on the device lifetime, without losing connectivity with the base station.

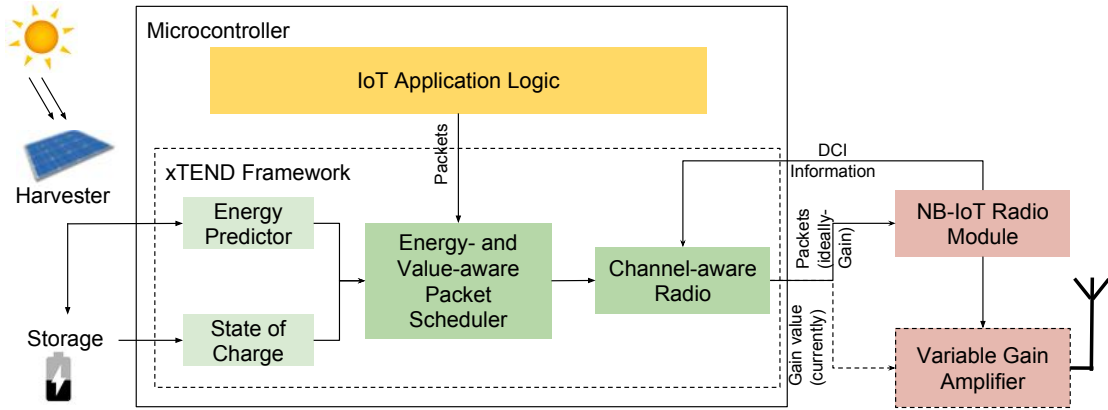


Figure 1.2: Block diagram of the xTEND framework in a UE

1.2. METHODOLOGY

To meet the set research objective, in this work, ambient energy-harvesting (EH) techniques that augment the battery of a UE are adopted. EH techniques have been investigated well in the context of wireless sensor networks (WSNs) and the Internet of Things [16]. However, commonly developed techniques such as adaptive duty cycling of the device do not work due to the signaling overhead associated with each attempt of connection to the base station, once the connection is lost when the device is forced to a sleep state. Further techniques such as adapting the transmission power of the device are not allowed, as the base station determines the transmission power of the device based on the channel conditions. Furthermore, the spatiotemporal variations of the ambient sources lead to low amounts of energy harvested. To this end, we propose the xTEND (eXtending the lifeTime through Energy-harvesting for NB-IoT Devices) framework as a middleware between the application layer and the radio. The xTEND framework, as shown in Figure 1.2, considers the harvested energy and the available energy to schedule the transmission of a packet and amplifies the transmitted signal if required. The energy- and value-aware packet scheduler (EVAPS) block models the scheduling problem as a 0/1 incremental knapsack problem, wherein the available energy is the size of the knapsack, weight of the packet is the energy that is required for transmission, and the value of the packet is the priority of the data. We consider that any IoT application will generate packets of different priorities, e.g., with a parking sensor on a UE in the smart-parking use-case, the house-keeping data may have low priority, sensor data may have mid priority and an event (i.e., cars entering or leaving the zone) may have the highest priority. A light-weight online policy for the scheduler is derived.

A second innovation proposed is a channel-aware radio that reduces the time required for a payload transaction¹, in turn energy consumption, by adapting the gains of a power amplifier. The channel-aware radio (ChAR) block is particularly developed for deep coverage scenarios where the transmission duration is expensive due to higher transmission powers and longer transaction times due to frame repetitions. ChAR block reads the debug information from the NB-IoT block to identify and decide whether to amplify the signal or not. The xTEND framework as a whole will not only extend the cumulative value of the generated packets with highly energy-efficient payload transactions but will also increase the scalability of the NB-IoT network due to shorter transaction times.

¹We use the term transaction to refer to the whole process that spans from the UE waking up from PSM mode, sending signaling information, obtaining a slot, transmitting the data, receiving the ACK, performing the cDRX operation, performing the iDRX operation, to the device reentering the PSM mode.

1.3. CONTRIBUTIONS

Specifically the contributions in this work are as follows.

1. With the UE and the power monitoring device, the NB-IoT transactions in various coverage scenarios and at various locations are characterized. A detailed energy consumption model is formed.
2. Based on real-world energy harvested datasets for indoor and outdoor ambient light, a feasibility study for adopting energy harvesting in NB-IoT is performed.
3. The xTEND framework is proposed that maximizes the time to depletion of the battery augmented with energy-harvesting capabilities. The framework is designed to work with no changes in the NB-IoT stack.
4. In the xTEND framework, the packet scheduling problem is modeled as a 0/1 knapsack problem. This work proposes a low-complexity, scheduling policy that outperforms an online algorithm that has a constant approximation of $1 + \ln(\frac{U}{L})$, where U and L are the upper and lower bounds for the value to weight ratio.
5. The channel-aware radio block is implemented on the UE and its performance is evaluated. It was observed that, on an average, energy can be reduced by 3.8 J and the total transaction time by 8.027 s due to the reduction in repetitions in deep coverage scenarios.

1.4. ORGANIZATION

This thesis is organized as follows: Chapter 2 provides a brief description of NB-IoT and present the related literature for NB-IoT, EH and related energy management techniques. Chapter 3 models the energy consumption of an end-to-end transaction and performs energy characterization for different coverage conditions and payload sizes. Further, the device lifetime estimations are provided in the section. In Chapter 4, the proposed framework is presented and the performance evaluation of the framework is done in Section 5. The conclusions and future work proposals are presented in Chapter 6.

2

BACKGROUND & RELATED WORK

This chapter presents a detailed account on the NB-IoT radio technology, the physical radio transactions and a step by step transition between modes when a device is powered up and exchanging data. This includes modes provided in the standards to reduce energy consumption. Further, the related literature in NB-IoT, EH and energy management techniques are investigated.

2.1. PHYSICAL LAYER: A SHORT OVERVIEW

The physical layer consists of physical channels and signals, that enable the exchange of control and scheduling information, synchronization information, and payloads between the sensor device and the cellular base station. In practical deployments, the NB-IoT technology can be deployed with the existing network in three different modes: using a frequency band in the LTE bandwidth (in-band mode), in the guard bands of the LTE network (guard band mode) and by re-farming a part of the GSM spectrum (in stand-alone mode), as shown in Figure 2.1. The network accessed for this work provides NB-IoT technology in the in-band mode of deployment.

2.1.1. A FRAME LEVEL PERSPECTIVE

In the in-band mode of deployment, within the LTE bandwidth, the NB-IoT carriers occupy a 180 kHz of allotted frequency space. This space is utilized to perform operations such as cell selections, uplink and downlink transactions, synchronization with base stations etc., performed by a set of physical channels and signals. The carrier frequency that carries signals to perform cell selection is the anchor carrier [3]. The information is carried in the time-frequency spectrum, which can be sorted as slots/-

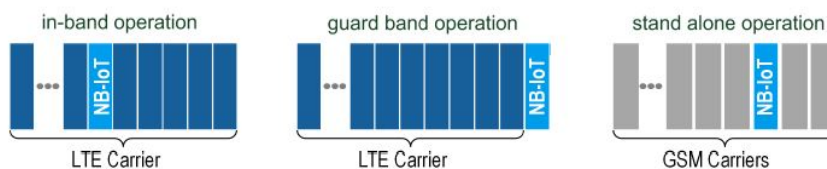


Figure 2.1: the different deployment modes [2] of NB-IoT

physical resource blocks, subframes, frames, and hyperframes. A unit of 1 ms (two consecutive slots) in time and 180 kHz in frequency is termed as a Physical Resource Block (PRB) pair. A set of ten consecutive PRB pairs constitute a subframe. Similarly, ten consecutive subframes make up a frame and 1024 consecutive frames make a hyperframe. Any two pairs of subframes, frames, and hyperframes have zero intersection. Figure 2.2 shows the radio frame structure.

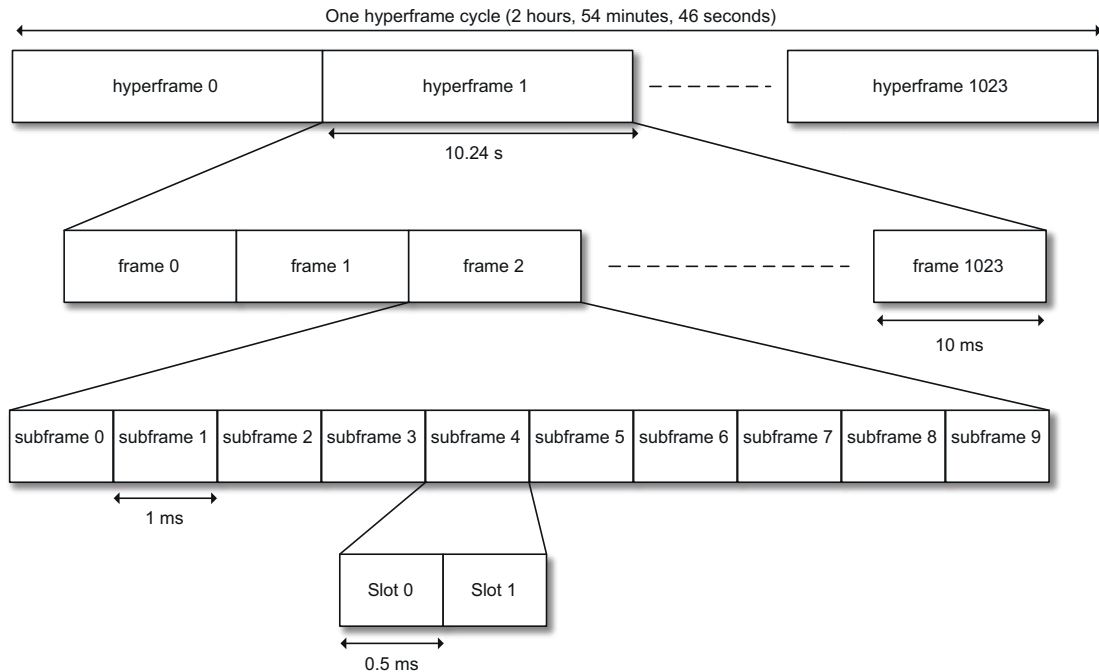


Figure 2.2: Frame-level structure [3] representing the slot, subframe, frame and hyperframe

Further, each PRB is subdivided in frequency into subcarriers. In the downlink, the smallest division (for scheduling) of a subcarrier is 15 kHz. The multiple access scheme used in the downlink is the Orthogonal Frequency-Division Multiple Access (OFDMA). Each PRB consists of 14 OFDM symbols. By this scheme, data is modulated on to the orthogonal subcarriers, mitigating the effects of intersymbol interference from the neighboring symbols. Unlike the downlink, the uplink transmissions allow sub-PRB level bandwidth allocations [3], that benefit in terms of radio resource usage (bandwidth saved) and energy savings (brings in close to 0 dB peak to average power ratio), and can still satisfy the small data packet requirements of the application. The uplink supports multi-tone (groups of sub-PRB level divisions) and single-tone frequency (single sub-PRB level division) utilizations for transmissions. The smallest schedulable quantity in the uplink is termed as a Resource Unit (RU) and depends on whether the deployment uses multi-tone or single tone operations. In the multi-tone operations, an RU can be defined as a subcarrier division of 180 kHz with 1 ms duration (2 slots) or 90 kHz with 2 ms duration (4 slots) or 45 kHz with 4 ms duration (8 slots) or 15 kHz with 8 ms duration (16 slots). Single-tone defines two terminologies for slots: 15 kHz subdivision in frequency (where a slot is 0.5ms in duration) and 3.5 kHz subdivision in frequency (where a slot is 2 ms in duration). The network, on which this work is based on, provides a single tone operation with the 15 kHz terminology. In the uplink transmissions, Single Carrier-Frequency Division Multiple Access (SC-FDMA) scheme is used, which helps reduce the peak to average power ratio of the transmitted waveform. This reduces the power back-off from the maximum possible transmission power, and hence saving battery lifetime.

The NB-IoT device performs Half Duplex - Frequency Divided Duplex to perform data exchange. This implies that the device performs transmission and reception activities in different frequencies, performing either of the two at a time. The type of modulation scheme used in the data exchange de-

depends on the direction of transmission and the number of tones used for transmission, with QPSK being the highest modulation scheme.

2.1.2. PHYSICAL CHANNELS, PHYSICAL SIGNALS, AND SCHEDULING IN TIME-FREQUENCY FRAME

There are 3 physical downlink channels and 2 physical uplink channels. The downlink channels are :

1. **Narrowband Physical Broadcast Channel (NPBCH):** This channel carries the Master Information Block (MIB) that holds information such as: the deployment mode, frequency raster offset, System Information block 1 (SIB1-NB) related information such as the size of the block and repetition count etc.
2. **Narrowband Physical Downlink Control Channel (NPDCCH):** This channel carries the Downlink Control Information (DCI), that holds the information to the devices about - the uplink grant to transmit payload (DCI-N0), the downlink scheduling from the eNB (DCI-N1) and the paging information from the network (DCI-N2). An NPDCCH search space defines a set of sub-frames that could possibly hold the DCI for the device. The device utilizes the Radio Network Temporary Identifiers (RNTI) to look into these search spaces and decodes the NPDCCH if its RNTI can unmask the search space.
3. **Narrowband Physical Downlink Shared Channel (NPDSCH):** This channel carries the downlink data from the eNB, including the System Information Blocks (SIBs) and the payload (as transport blocks) from the network. Transmission gaps can be configured to avoid blockage due to a specific device if a large number of repetitions are required. The maximum transport block size in the downlink is 680 bits.

When a device wakes from sleep after a long time, the timer value it has would probably be incorrect with considerable frequency offset. Hence, apart from the physical channels, there are two synchronization signals in the downlink. They are :

- **Narrowband Primary Synchronization Signal (NPSS):** The signal provides synchronization to both time and frequency. The device correlates a known NPSS signal with the received signal.
- **Narrowband Secondary Synchronization Signal (NSSS):** The signal helps to identify the Physical Cell ID (PCID, unique to a base station) and the frame structure.

In the Uplink, the physical channels are:

1. **Narrowband Physical Random Access Channel (NPRACH):** This channel is used by the device to initiate a connection by sending a preamble. A preamble consists of symbol groups with a basic repetition unit of 4 symbol groups. Each symbol group is made of a cyclic prefix followed by 5 SC-FDMA symbols. Within a repetition unit, the tone frequencies of the symbol groups follow a pre-determined tone hopping pattern. The frequency hopping between the symbol groups allows the base station to identify the Time of Arrival (ToA) and hence, determine the Timing Advance (TA) for each device. This helps to align received frequency multiplexed signals from different devices and preserve orthogonality between them[3]. Three NPRACH configurations are supported corresponding to different coverage classes.
2. **Narrowband Physical Uplink Shared Channel (NPUSCH):** carries the uplink payloads (called as NPUSCH Format 1) and the Hybrid Automatic Repeat Request (HARQ, called as NPUSCH

Format 2) acknowledgments, send upon reception of a payload at the UE. The maximum transport block size in the uplink is 1000 bits.

Additionally, there are reference signals: the NRS (in downlink) and the DMRS (in uplink), that provide information about the channel conditions, at their destinations. NPDCCH, NPDSCH, and NPUSCH carry the information bits for the payload exchange between the UE and the eNB. Each of these channels occupies one subframe at the minimum. Further, repetitions of subframes along with coding rate, which is the ratio of the information allocated in a subframe to the maximum information that can be allocated, is the technique utilized to improve coverage. NPDCCH and NPDSCH can be repeated up to 2048 times and NPUSCH can be repeated up to 128 times, in the worst case. Further, a single NPDSCH can be mapped to 10 subframes. In the uplink, an RU with subcarrier frequency length of 3.75 kHz has 16 slots, implying a duration of 32 ms as per the 3.75 kHz terminology. This implies that, in the worst case, a single NPDSCH could occupy 20480 subframes and an NPUSCH could occupy 4096 subframes, with the time spend on them is even longer due to other channels, scheduling delays etc. The high number of repetitions and low coding rate would mean longer durations for the transaction.

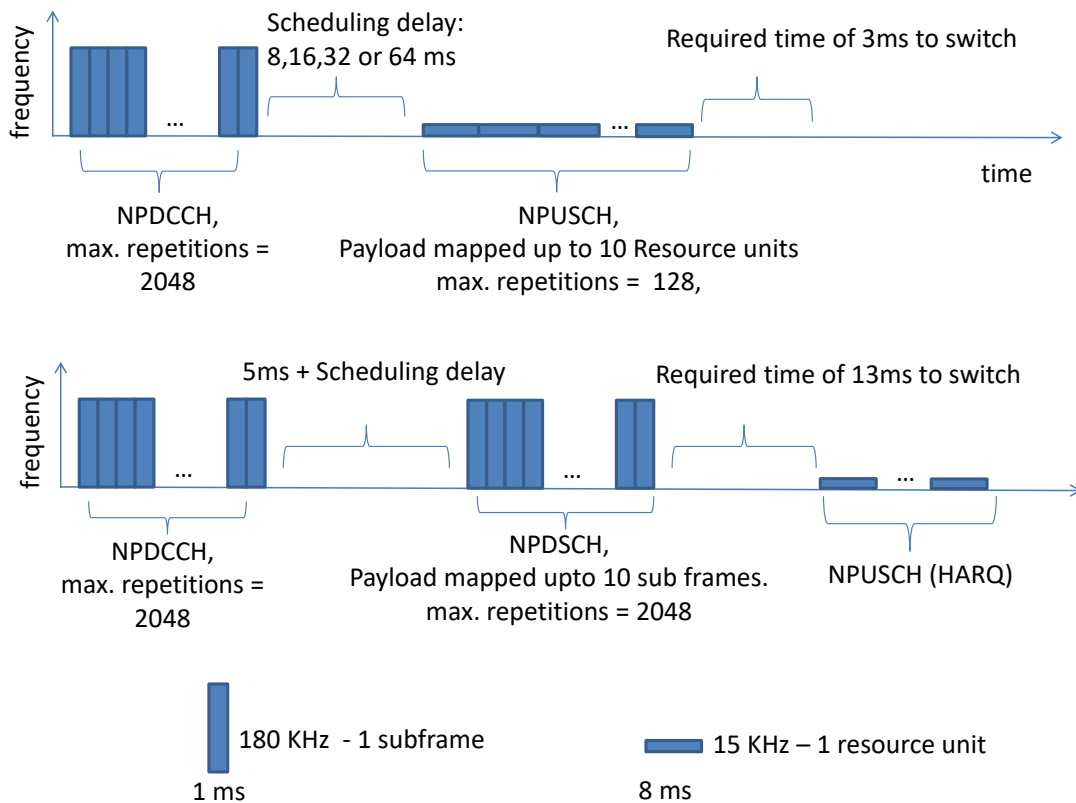


Figure 2.3: Scheduling of transport blocks in the uplink and downlink

The scheduling in the uplink and the downlink in a time-frequency spectrum is presented in Figures 2.3. In the uplink scheduling, the resource units for NPUSCH are short and wide to represent the sub-PRB frequencies utilization of 15 KHz, with one slot being 8 ms wide in time.

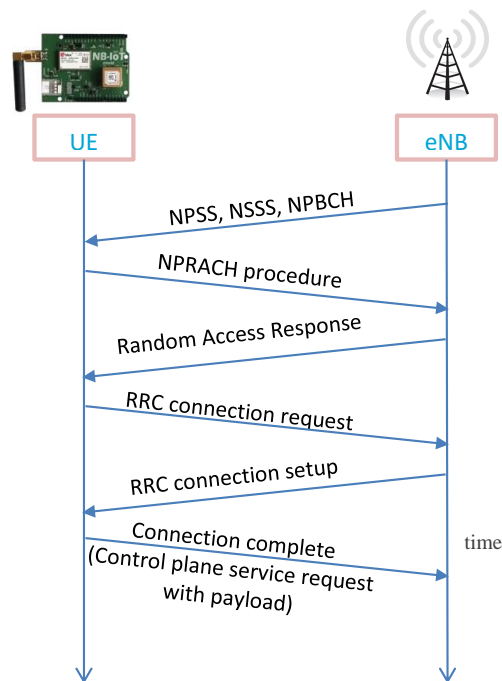


Figure 2.4: A payload exchange procedure between the UE and the base station

2.2. PHYSICAL TRANSACTIONS IN NB-IOT

An NB-IoT device transits through different modes as it boots up connects to a base station and performs payload exchanges. In this section, these modes and the transitions among them are briefly described. Further, the solutions in the standards to reduce energy consumption in the devices are also presented.

2.2.1. ATTACH PROCEDURE: WHEN THE DEVICE POWERS UP

When an NB-IoT device is powered up, it needs to register with the network by setting up a radio connection with an eNB. However, a time-frequency offset may exist between the UE and an eNB. The downlink physical synchronization signals - NPSS and NSSS - helps to synchronize. The device listens to NPSS and synchronizes with the base station in time, and then uses the signal to perform carrier frequency offset estimation. The device then identifies the NSSS subframes to use the signal information to identify the PCID and synchronize with the frame structure. The placements of NRS resource elements, within a subframe, are determined by the PCID. Upon acquiring synchronization, the device knows the location of the NPBCH channel in the frame structure and can decode it. Acquiring the MIB by decoding the NPBCH implies that the device can identify the location of the SIB1-NB available in the NPDSCH channel. With the acquisition of SIB1-NB, the device now can entirely identify the frame structure, the cell identity, information about other system information blocks etc. Thus, upon completely identifying the cell, the device compares against a set of threshold parameters to determine cell suitability and checks for access barring for the particular cell.

The UE performs a coverage class estimation and initiates the attach procedure by sending out a random access preamble in the physical uplink channel - NPRACH. Upon detection of a preamble, the eNB responds with a Random Access Response (RAR) containing scheduling information for the de-

vice to send the 'rrcConnectionRequest'. Upon receiving a connection request, the eNB resolves any contention between devices sending the same preamble and sends the 'rrcConnectionSetup' message, which is followed by the UE sending the 'rrcConnectionSetupComplete' Attach request message [3]. The device moves into connected state at this point. But the UE is not yet registered to the Mobility Management Entity (MME). The eNB forwards the Attach request to the MME, which enquires with the Home Subscriber Server (HSS) for the identity of the UE, and sends an Authentication request to the UE. The UE sends an authentication response with some parameters. Upon successful comparison of the parameters, the UE is authenticated. Further, the MME forwards a security mode command to the UE, with information regarding the ciphering and integrity protection to the UE. The UE confirms the command with a security mode complete message. This is followed by the Attach accept message from the network indicating to the UE the acceptance of the Attach request and provides the ACTIVATE_DEFAULT_EPS_BEARER_CONTEXT_REQUEST. The UE sends this request to the ESM sublayer, and once it is established, the UE replies with an Attach complete message. With this, the device is registered with the MME. If no activity is detected, the device moves into the idle state with the expiration of appropriate timers.

2.2.2. SOLUTIONS IN THE STANDARDS TO REDUCE ENERGY CONSUMPTION

An NB-IoT device, serving infrequent data exchanges (as is mostly required of it), spends very less time in active transactions. Hence by duty-cycling the operations of the device, much energy can be saved while still serving the application. The standards describe different modes that provide different duty-cycling periods and dictates the transition from the active mode to these modes. Discontinuous Reception (DRX) is a mode that enables to duty cycle the monitoring of the paging operation during the connected (connected mode DRX) and idle mode (idle mode DRX), whereby the reception activity to check for paging happens once every DRX period (a maximum of 10.24 sec). The device can move into the DRX mode from the active mode if there are no transactions between the device and the base station. In NB-IoT, only long DRX mode is made available [17]. The device upon completing the long-DRX period moves into the idle state and performs idle mode DRX operations.

Apart from the normal DRX operations, the 3GPP standards specify two modes that provide further increased sleep time - the enhanced DRX mode (eDRX) and Power Saving Mode (PSM). The eDRX mode allows the sleep time to be extended up to 2 hrs. 54 min and 46 sec, after which the paging operations occur with the predetermined idle mode DRX period. This continues up until a set paging transmission window after which the device enters the next eDRX period and goes to sleep [3]. The PSM enables the UE to remain in sleep for a much longer period. The UE sends the timer values it requires for PSM and eDRX, to the eNB, in the 'Attach request'/'Tracking Area Update (TAU) request' RRC messages. If the values fall within the boundaries configured by the network, the timer values are accepted in the 'Attach accept'/'Tracking area update accept' RRC messages. To switch on to the PSM, the 'Active timer T3324' has to expire, which is set when the UE moves into the idle state. The UE continues to remain in this state until the 'T3214 Extendedvalue timer' expires, upon which a TAU request is send [3]. The power consumption during the PSM mode corresponds to the current consumed by a low power crystal, few active circuitry and due to leakage, and is typically 0.015 mW [8].

2.2.3. PAYLOAD EXCHANGE PROCEDURE

As the device wakes up from sleep, due to an event occurrence or periodic sensing, the UE raises a control plane service request and follows the same initial steps as the attach procedure to set up the radio link (setting up of the RRC connection). In order to reduce signaling overheads due to the setup of data radio bearers, as is done in the existing LTE network [3], a control plane optimization is proposed which piggybacks short and infrequent messages as a part of the Non-Access Stratum (NAS), 'rrcConnectionSetupComplete' message. This eliminates the signaling overheads required to

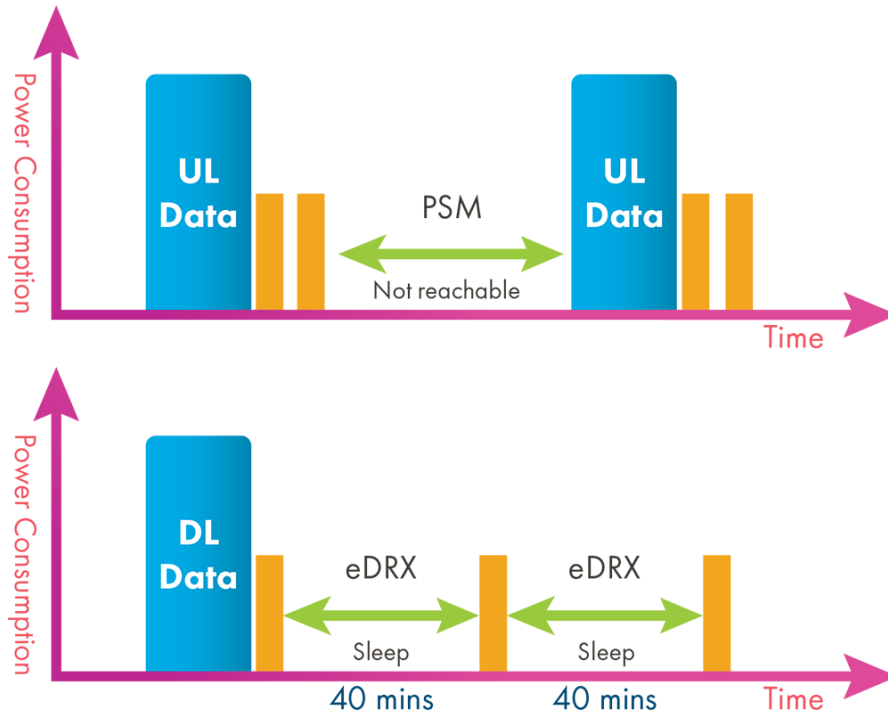


Figure 2.5: PSM and eDRX procedures. The eDRX cycle can extend up to 175 min. [4]

set up the data radio bearers, as is done in the existing LTE network [3]. Once the device completes its transactions (uplink and downlink) it moves into the connected mode DRX and then into idle mode performing idle mode DRX, upon expiry of respective timers. If PSM is configured, the device moves out into PSM upon the expiry of the 'Active timer' which is set when the device moves into the idle mode. Else, the device remains in the idle mode. Figure 2.4 shows the ladder diagram for a payload exchange procedure.

2.3. RELATED WORK

The relevant literature is categorized into NB-IoT related and energy-harvesting related works.

Work on NB-IoT. Instances of energy consumption models and performance analysis of NB-IoT devices exist in the literature. Lauridsen, M et. al. [13] models an end to end payload transaction and provides the power consumption measurements performed on two NB-IoT devices and their lifetime estimations. The authors state that the devices would last 21- 85% shorter than the expected projections. The model, however, does not consider a downlink reception and the corresponding HARQ transmissions. Further, the lifetime estimations are performed with a 27.7 Wh battery with a safety factor of 0.66 in the estimations. Martinez et. al. [18] evaluates metrics such as energy consumption, delay tolerance, uplink, and downlink power consumption. The energy consumption of a UE under different coverage conditions, with different packet sizes with variable network configuration such as the Inactivity timer, Active timer etc. is empirically obtained for a sizable dataset. The results indicate a mean lifetime of 2-3 years with a 1Ah energy buffer and reporting rate of 1 message per hour. However, in this case, the measurements are performed for an SNR range from 0 to 140 dB and not further below this range where the coverage enhancements would have a larger impact on the device lifetime. M. El. Soussi et. al. [19] formulates an optimization problem to reduce the energy consumption during an eDRX/PSM period. To this end, a power consumption model is proposed for computing the device

lifetime comprising of the different events that occur during message transactions. Based on theoretical parameters lifetime estimations are performed. Similarly, performance analysis and lifetime estimations with theoretical values for different traffic distribution are available in the literature [3, 20]. In this work, empirical power measurements are presented for different coverage conditions, which includes deep coverage where there is a maximum impact of the coverage enhancements on the device lifetime. The measurements provide an energy matrix which forms a rough estimate for payload transactions in a coverage condition. Further, unlike the aforementioned works, an end-to-end energy consumption model at a physical channel level is modeled, and the device lifetime is computed. Finally, lifetime estimations and comparisons to expectations in the standards are provided.

Further, work aimed to reduce energy consumption in NB-IoT devices are present in the literature. In [21], the authors propose the use of maximum-likelihood detectors in place of the auto-correlation detectors, indicating an energy saving in initial timing acquisition of up to 34%. The suggested low latency detectors, however, have high computational complexity as a trade-off. Schemes for performing effective link adaptation, also considering the number of repetitions factor, in uplink and downlink is presented in [22] and [23], respectively. The results indicate savings in resource usage and energy consumption. In [24], the authors suggest an innovative DRX strategy for a deployment with a large number of devices that are separated as groups. Each group is identified by an ID and a group leader, which wakes up more often than the other devices in the group during paging. Further, the group ID is used to mask scheduling information for a group, hence making efficient use of radio spectrum. The energy savings are obtained with the trade-off of latency. In this work, due to inaccessibility to the NB-IoT stack or the intelligence in the base station, the work is confined to the application layer and the hardware of the device.

Work on Energy-harvesting. The challenges related to energy-harvesting have been well studied in the literature. This includes multi-source harvesting systems [25] for devices exposed to less ambient energy and directions on choosing efficient harvesters, appropriate storage and low-power hardware devices [25, 26]. In the domain of schemes that perform intelligent energy management of the harvested energy, an extensive amount of literature exist in the context of wireless sensing networks (WSN). However not all these solutions are directly applicable in NB-IoT enabled applications. For instance, duty cycling of the system functionalities (sensing, payload transmissions) and adapting the application rate (the rate at which the sensed payloads are transmitted) [27] based on the energy availability is a common energy-management scheme [28, 29]. However, transactions in existing NB-IoT deployment require the establishment of radio link connections between the device and the base station. Duty cycling would result in additional energy losses due to the frequent signaling procedures. Further, depending on the source of the payloads or the ambient energy a substantial amount of methodologies exist in the literature to perform efficient energy management. Both the harvesting source and the payload source can be represented using stochastic distributions or as a deterministic model. Stochastic systems can be modeled using the well established Markov Decision Process (MDP) framework. A detailed survey on the use of the MDP framework in the context of WSNs is presented in [30]. Different variants of the framework are used depending on the problems dealt with. Lei et al. [31] propose an optimal transmission policy for WSNs based on the MDP framework that maximizes the average reward rate. The model performs a value-based scheduling of the messages, and both energy-harvesting arrivals and the payload arrivals are modeled as a stochastic distribution. Shaobo Mao et al. [32] considers both the sensing and transmission energy and seeks to maximize the average throughput by defining a sequential decision problem in a finite horizon. Only the incoming energy is modeled in a stochastic distribution and the model does not perform value-based scheduling. Nicol'o et al. [33] proposes a low-complexity transmission policy that maximizes the average importance of the reported data. The model performs value-based scheduling and adapts the transmission probabilities according to the harvesting states. For deterministic models, that know precisely about the energy arrivals and messages arrivals, transmission policies can be computed offline.

In this work, effective energy management is implemented via a lifetime extension framework. The framework translates the problem of scheduling payload exchanges of an NB-IoT device as a knapsack problem. The knapsack problem, in its many alterations, has been well studied and researched in the literature. Incremental knapsack problem was investigated by Bienstock et. al. [34]. The authors provide a constant factor approximation scheme for a time-invariant incremental knapsack problem. Incremental knapsack problem in the context of energy harvesting is presented in [35], with online threshold-based schemes for stochastic and deterministic knapsack problems and presents comparisons for varying weights and values of the knapsack items. The authors extend a threshold scheme for static capacity online knapsack problem, with a competitive ratio of $1 + \ln(\frac{U}{L})$ (where U and L are upper and lower bounds of the value-weight ratios), to dynamic capacity scenarios. This scheme (Jumping threshold) is used for comparisons to the threshold based solution proposed in this work.

3

ENERGY CHARACTERIZATION AND EH FEASIBILITY STUDY

In this Chapter, the energy characterization of an NB-IoT UE device is performed in different coverage conditions. The current traces are analyzed and the current consumed during different activities such as transmission and reception are identified. The lifetime of a UE is estimated and compared against the standards. A feasibility study of incorporating energy-harvesting technology is performed, and the challenges are identified.

3.1. ENERGY CHARACTERIZATION

In this section, the energy consumption measurements of an NB-IoT device engaged in a payload transaction is obtained based on empirical measurements under different coverage conditions. The measurements are performed on a real-world NB-IoT deployment. Based on the energy measurements, this work models the energy consumption of a device. With the required parameters, the equations would suffice to perform a static calculation of the device energy consumption for a payload transaction, for the given coverage condition.

3.1.1. ENERGY MEASUREMENTS

EXPERIMENTAL SETUP

The experiment setup is shown in Figure 3.1. The measurements are obtained with the U-blox evaluation board - EVK-N2 - containing the SARA N211 radio modem [14]. Two such U-blox devices were used to take the measurements. Apart from the NB-IoT stack, the device consists of the UDP and IP stacks. No additional application layer is used for the transactions. For the energy consumption measurements and lifetime estimations, a 130 bytes payload (200 bytes in packet size) is sent to a local server, that acknowledges the device with a 13 byte (65 bytes in packet size) payload data. The choice of the packet size in uplink and downlink is based on the selection of packet size made in the standards to perform lifetime estimations. The measurements are obtained using the power monitor from Monsoon solutions. The offsets due to the other power consuming circuitry were nullified and the measurements were taken. The power monitor device is used as the power supply to the radio modem with a constant voltage of 3.8 V. Analysis at the subframe level was performed using the Accuver

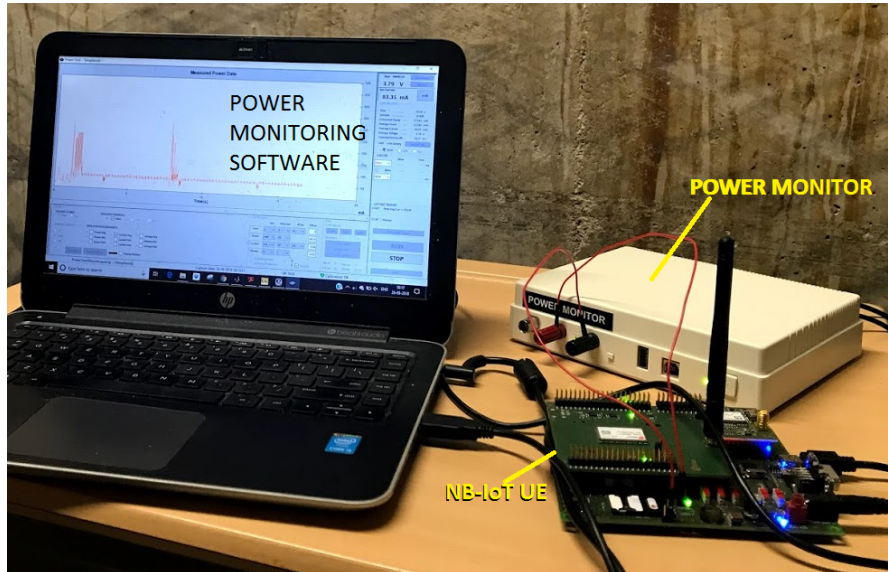


Figure 3.1: The experimental setup

XCAL tool. The NB-IoT device logs the messages exchanged in the ASN.1 specification which is then decoded using the XCAL tool.

The coverage conditions of different locations in the city of Delft where the measurements were taken

- -124 dB > RSRP > -136 dB
- -113 dB > RSRP > -124 dB
- -104 dB > RSRP > -113 dB
- -96 dB > RSRP > -104 dB



Figure 3.2: Map indicating locations in the city of Delft where the measurements were taken

ENERGY MEASUREMENTS

Figure 3.2 indicates the various locations in the map at which the measurements were taken and the corresponding coverage conditions in terms of the RSRP (Received Signal Received Power). For a given coverage condition and payload size, the measurements are performed at least 20 times, and then the average is computed. The measurements correspond to the energy consumption cost of payload exchanges, as the device wakes up from PSM, performs the payload exchange in the Active mode, moves into the connected DRX, idle mode and finally moves into PSM. The measurements are presented in Figure 3.3 and the following observations can be drawn:

- On an average, the energy consumed by a device in -124 dB > RSRP > -136 dB range is 20.59 J, -113 dB < RSRP < -124 dB range is 6.31 J, -104 dB < RSRP < -113 dB range is 3.96 J, and -96 dB < RSRP <

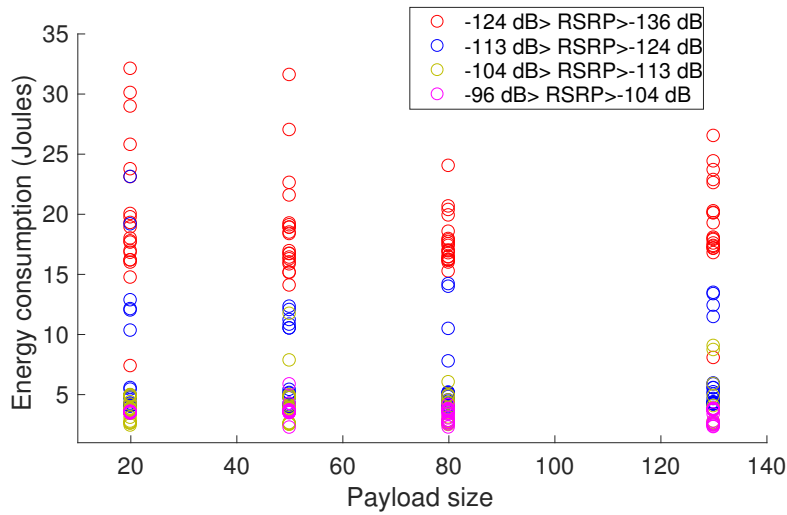


Figure 3.3: Energy consumption measurements for different payload sizes for 4 different coverage conditions

-104 dB is 3.091 J.

- As the coverage worsens, the device energy consumption increases due to the coverage enhancement techniques.
- On an average, the difference between the energy consumption of different payload sizes do not vary much. The difference in the energy consumption between the different payloads is not much in comparison to the total energy consumption of the device.

3.1.2. ENERGY CONSUMPTION MODEL

Based on the energy measurements, the energy consumption of the device performing a payload transaction is modeled. The transaction is split into different stages: initial connection, transmission of transport blocks, reception of transport blocks, NPDCCH monitoring in Active mode, cDRX mode, iDRX mode, and the PSM. The different stages in a transaction is identified in Figure 3.4, and each component is described in table 3.1. Given that the transmission power is TX_{power} , the reception power is RX_{power} and the power consumed during the light sleep period in Active mode is LS_{power} , the energy consumption for each stage, as marked in Figure 3.4, is formulated.

Initial connection: The energy consumption for the initial connection consists of monitoring the NPSS and NSSS, and sending the preamble in the NPRACH. This can be presented as:

$$E_{In} = E_{ss} + E_p$$

where,

- E_{ss} is the energy required to monitor the NPSS and NSSS signals.
- E_p energy consumption for the NPRACH procedure defined as: $TX_{power} \times \text{Number of repetitions} \times \text{Basic unit (5.6/6.4 ms)}$

Transmission: A transmission procedure consists of reception of the uplink grant in the NPDCCH and transmitting a transport block in the NPUSCH. The total time taken for a transmission in NPUSCH is

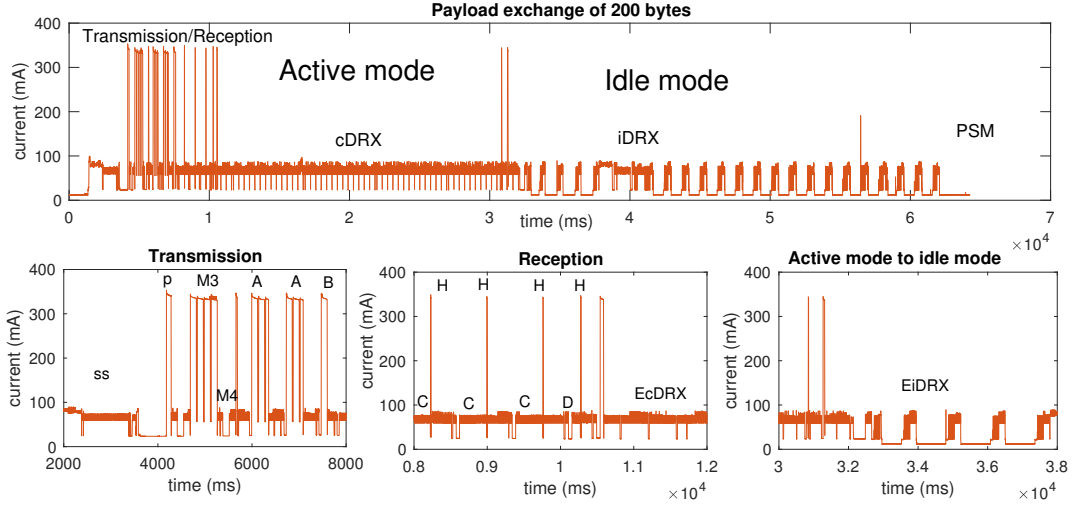


Figure 3.4: The current trace for a payload exchange obtained using the power monitor. The transmission, reception and idle mode stages are presented separately in row 2.

SS	P	M3	M4	A	B	C	D	H
Monitoring NPSS and NSSS signals	NPRACH preamble	RRC Connection Request (Message3)	RRC Connection Setup (Message 4)	TX 1000 bits	TX 308 bits	RX 608 bits	RX 208 bits	HARQ transmission

Table 3.1: The different components in the active mode of a message transaction

based on the repetition numbers allocated, the number of subframes the transport block is mapped to and the number of tones in the uplink. The energy consumption during transmission of a transport block can be modelled as:

$$E_{TX} = E_{DCIN0} + E_{NPUSCH} + E_{TX-SD}$$

where,

- E_{DCIN0} is the energy consumed by the device for the reception of the DCI for uplink grant. It can be defined as: $RX_{power} \times \text{Number of repetitions of DCI-N0} \times 1 \text{ ms}$,
- E_{NPUSCH} is the energy consumed by the device for the transmission of the transport block. It can be defined as: $TX_{power} \times \text{Time for a single RU} \times \text{Number of repetitions} \times \text{Number of subframes} \times 1 \text{ ms}$.
- E_{SD} is the energy consumed by the device in light sleep during the scheduled delay between the NPDCCH and NPUSCH. It can be defined as: $LS_{power} \times SD_{TX}$

Reception: A reception procedure consists of the reception of downlink scheduling information in the NPDCCH, the downlink transport blocks in the NPDSCH and transmitting the uplink HARQ in the NPUSCH. The energy consumption during the reception of one transport block can be modelled as such:

$$E_{RX} = E_{DCIN1} + E_{NPDSCH} + E_{NPUSCH-E} + E_{RX-SD}$$

where,

- E_{DCIN1} is the energy for the reception of the DCI for downlink scheduling. It can be defined as: $RX_{power} \times \text{Number of repetitions of DCI-N1} \times 1 \text{ ms}$,
- E_{NPDSCH} is the energy consumed by the device while receiving a transport block in NPDSCH. It can be defined as: $RX_{power} \times \text{Number of repetitions} \times \text{Number of subframes} \times 1 \text{ ms}$,
- $E_{NPUSCH-F2}$ is the energy consumed in transmitting the HARQ acknowledgement in the NPUSCH. It can be defined as: $TX_{power} \times \text{Number of repetitions} \times \text{Time for a single RU}$
- E_{SD} is the energy consumed by the device in light sleep during the scheduled delay between the NPDCCH and NPDSCH, and the NPDSCH and NPUSCH-F2. It can be defined as: $LS_{power} \times SD_{RX}$

Connected mode DRX: The energy consumption during cDRX mode can be modelled as such:

$$E_{cDRX} = E_{on} + E_{off}$$

where,

- E_{on} is the energy consumed during the paging operation in the cDRX mode. It can be defined as $RX_{power} \times \text{Inactivity timer period} \times \delta_{cDRX}$, where δ_{cDRX} is the ratio of ON period to OFF period configured for the cDRX operations.
- E_{off} is the energy consumed during the OFF period in the cDRX mode. It can be defined as $LS_{power} \times \text{Inactivity timer period} \times (1 - \delta_{cDRX})$, where δ_{cDRX} is the ratio of ON period to OFF period configured for the cDRX operations.

Monitoring NPDCCH: The device spends energy in monitoring the NPDCCH in between the transmission/reception activities. The energy consumption due to this can be modeled as such:

$$E_{NPDCCH_mon_active} = |RX_{power} \times (\text{Abs.Time}_{TX_{final}} - \text{Abs.Time}_{TX_1} - \sum \text{Time}_{TX} - \sum \text{Time}_{RX}) - E_{cDRX}|$$

where,

- $\sum \text{Time}_{TX}$ represents the total time of all transmission procedures and $\sum \text{Time}_{RX}$ represents the total time of all reception procedures.
- Abs.Time_{TX_1} and $\text{Abs.Time}_{TX_{final}}$ represents the absolute time at the beginning of the first and the final transmission procedure.

Idle mode DRX: The energy consumption during idle mode can be modelled as such:

$$E_{idle} = RX_{power} \times \text{Active timer period} \times \delta_{iDRX}$$

The total device lifetime can be modelled as :

$$E_{device} = E_{In} + E_{TX_i} + E_{RX_j} + E_{NPDCCH_mon_act} + E_{cDRX} + E_{iDRX} \quad (3.1)$$

where,

- i varies from 1 to the total number of transmission procedures and E_{TX_i} corresponds to the energy consumed by the transmission procedure

- j varies from 1 to the total number of reception procedure and E_{RX_j} corresponds to the energy consumed by the reception procedure

Equation 3.1 presents the energy consumption model of a device engaged in a payload transaction. The equation is based on the empirical measurements, and hence, closely resembles the actual energy consumption.

3.1.3. LIFETIME ESTIMATION

In this section, device lifetime is estimated based on the empirical measurements made.

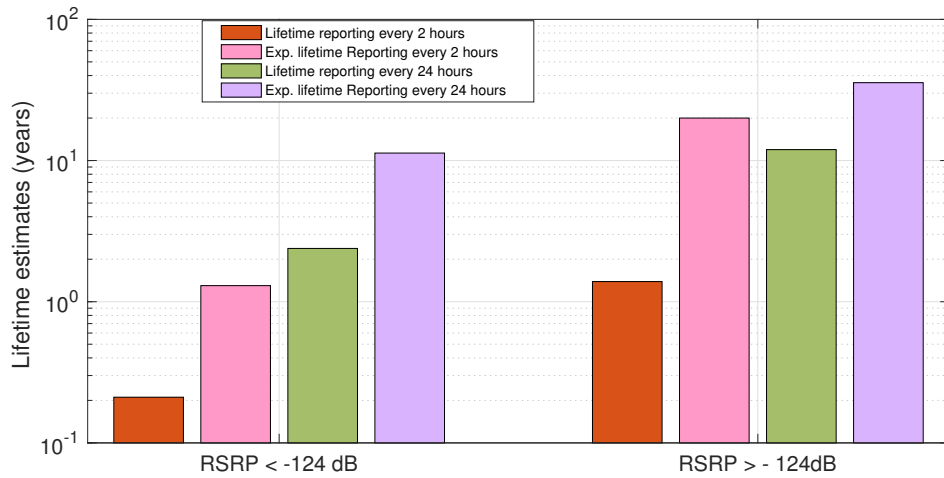


Figure 3.5: Lifetime estimations of the UE based on empirical measurements when compared to the expected measurements [3]

The estimation is performed considering a 5 Wh battery, which has also been considered in the 3GPP calculations [8]. The estimation is performed for a device that is engaged in a transaction where 130 bytes payload (200 bytes packet) is transmitted in the uplink and 13 bytes payload (65 bytes) is received in the downlink. Two reporting intervals are assumed for the lifetime estimations: once every 2 hours and once every day. The battery is assumed to provide a constant voltage source of 3.8 V, providing a charge of 1400 mAh. The estimations are made in two different coverage conditions: when the RSRP < -124 dB and when RSRP > -124 dB (specifically when -96 dB > RSRP > -104 dB, in the case of empirical measurements). The results of the lifetime estimations are presented in Figure 3.5. Based on the figure, the following observations can be drawn:

- The device does not meet the expected estimates in all the scenarios considered.
- The device lasts for 76 days and 2.38 years when the RSRP < -124 dB with a bi-hourly and a daily reporting interval, respectively.
- The device can meet the goal of 10 + years lifetime only when the coverage is such that RSRP > -124 dB, with a daily reporting interval.

The reasons for the significant differences in the empirical measurements to the expected lifetime estimations can be attributed to the following factors:

1. The difference in timer values such as the cDRX timer period, the Inactivity period etc. For instance, as observed from the Figure 3.4, the duty-cycling rate in the cDRX period is high, i.e., the device mostly remains in the reception mode during the Inactive timer period.
2. The transmission power measured is 1346.568 mW, and the reception power measured is 194.5 mW, when the RSRP < -124 dB. However, in the expected lifetime estimations [3], the transmission power is considered to be 500 mW (45% power amplifier efficiency, 60 mW for active circuitry and maximum transmission power of 23 dBm) in the deep coverage case, and 80 mW for reception.

It is observed that the lifetime of an UE device depends on the application's reporting rate and the coverage class. The reliability features (coverage enhancement techniques) in the NB-IoT standard such as high repetitions of sub-frames / resource units and low modulation and coding rates (MCS) used in the physical layer play a significant role when the coverage class of the device is in 'deep coverage' (RSRP < -124 dB). Hence, to meet the lifetime expectations in the standards, this work proposes to adopt energy harvesting techniques.

3.2. AMBIENT ENERGY TO THE RESCUE

Most deployment scenarios will not have accessible wired power sources for all the devices. Hence the devices depend on battery sources. By adopting energy-harvesting techniques, the devices gain autonomy with respect to energy. This also eliminates the laborious task of replacing the batteries. Of the several harvesting sources, the ambient light sources can provide higher power density [26]. NB-IoT devices deployed in a scenario can utilize the untapped ambient light energy sources (indoor and outdoor) in order to extend the *functional* lifetime (time to the first exhaustion of the battery) of the devices, .

3.2.1. ENERGY-HARVESTING PROFILES

In order to investigate the effectiveness of energy-harvesting with NB-IoT, we consider three sets of data: two corresponding to indoor conditions and one to an outdoor condition. For each set of data, we split a day into 24 periods, and average the energy obtained, as a measure of charge (mAh), throughout the year, for each period. For calculating the energy obtained from the harvester, we consider a harvesting area of 100 cm², a conversion efficiency of 15%, and a constant output voltage of 3.8V in all the cases. The variance is expressed by the error bars, in all three cases.

Indoor radiance measurements The data is obtained from the EnHANTS project, a study conducted in Columbia University [36].

Window sill: Figure 3.6 corresponds to the expected energy in a day, in terms of charge, obtained when the measurement device is placed on the window sill and shading is used.

Book shelf: Figure 3.7 corresponds to the expected energy in a day, in terms of charge, when the measurement device is placed on the bookshelf, away from the window such that the device receives direct sunlight for a short duration.

The bookshelf scenario has a broader graph in comparison to the window sill case due to constant indoor light, but with a reduced peak. The former is exposed to sunlight for a very short duration and hence has a low peak.

Outdoor radiance measurements The data is obtained from KNMI [37].

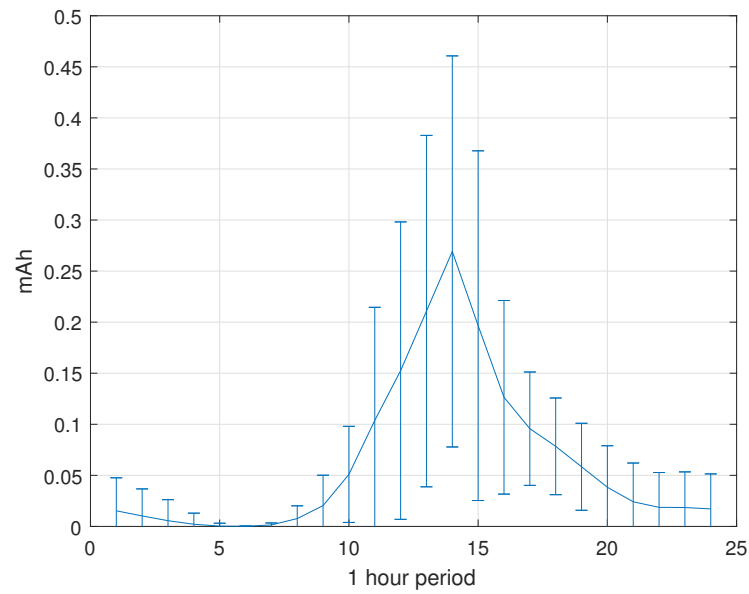


Figure 3.6: Window Sill - Averaged energy reading over 378 days for each 1 h period

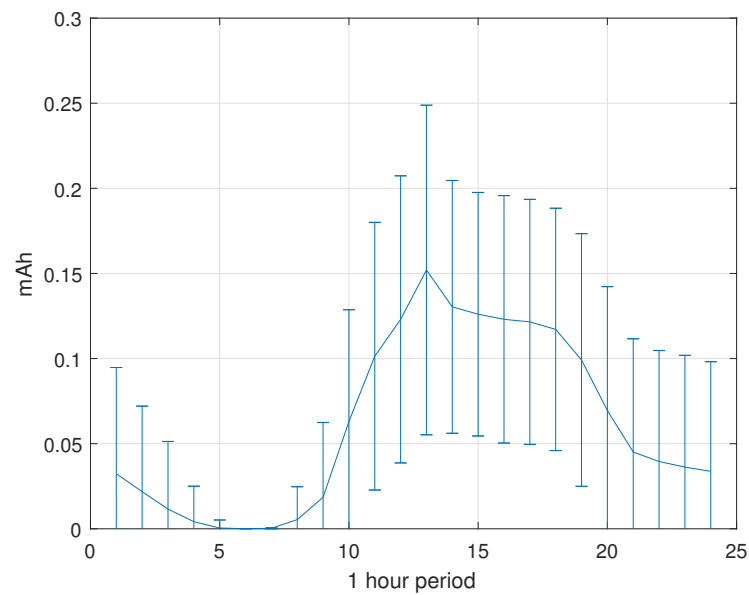


Figure 3.7: Book Shelf - Averaged energy reading over 341 days for each 1 h period

Outdoors: Figure 3.8 corresponds to the expected energy harvested in a day, in terms of charge, obtained in the city of Rotterdam for the entire year of 2017.

3.2.2. CONVERTING ENERGY INTO PACKETS

In this section, the average extension of the functional lifetime of a UE device whose battery is augmented with energy harvesters is computed for the same scenarios done in Section 3.1.3. Figure 3.9

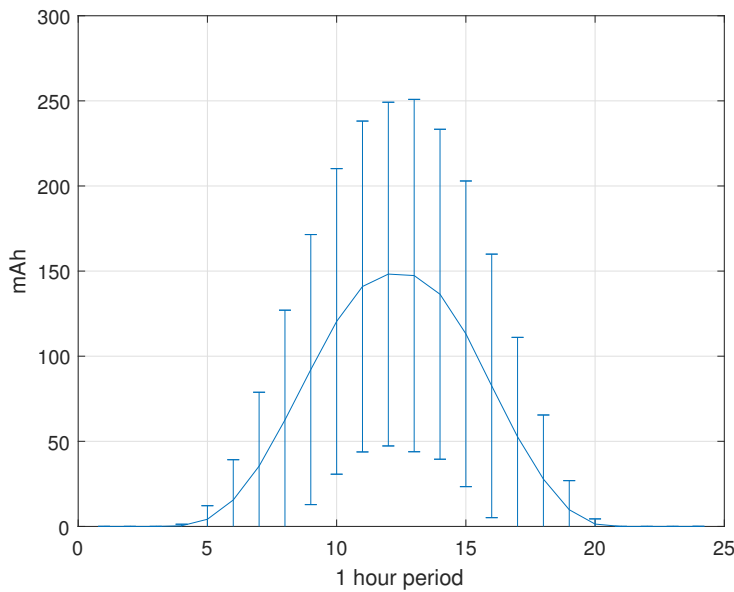


Figure 3.8: Outdoors - Averaged energy reading over 365 days for each 1 h period

represents the gain in energy obtained from the energy harvester, represented in terms of additional transactions (130 B uplink, 65 B downlink) that can be sent in a day/year, in two coverage conditions. Figure 3.9 indicates that the expected energy obtained in a day is just sufficient to serve one additional payload in ‘deep coverage’ conditions. However, with consumption rates such as 1 payload per day in ‘deep coverage’, the device can ‘ideally’ perform energy-neutral operations, for the indoor dataset. Further, we observe that by the given data sets, 50% and 87.4 % of the capacity of the battery considered, is obtained in a year in indoors and in a day in outdoor conditions, respectively. With a consumption rate of one payload per hour in our example above, the harvester can help serve the application for slightly more than 1.5 days, after which the transmission needs to stop to allow the battery to recharge.

3.3. CHALLENGES

In this section, a brief description of the challenges in energy-harvesting and inherent challenges in NB-IoT are presented. However, not all the challenges are addressed in this work.

3.3.1. CHALLENGES IN ENERGY-HARVESTING

Though energy-harvesting solutions are quite attractive, the technology has its fair amount of limitations, depending on various factors such as the harvesting source, the harvesting technology, the application, etc.

Incorporating energy-harvesting in IoT in general throws many challenges. We list them below.

1. *Design choice*: Determining suitable ambient energy sources for the given deployment scenario, the type of harvester (based on the ambient source, efficiency, application) and a suitable storage device (based on the location of deployment, capacity, duration of storage, leakage, etc).

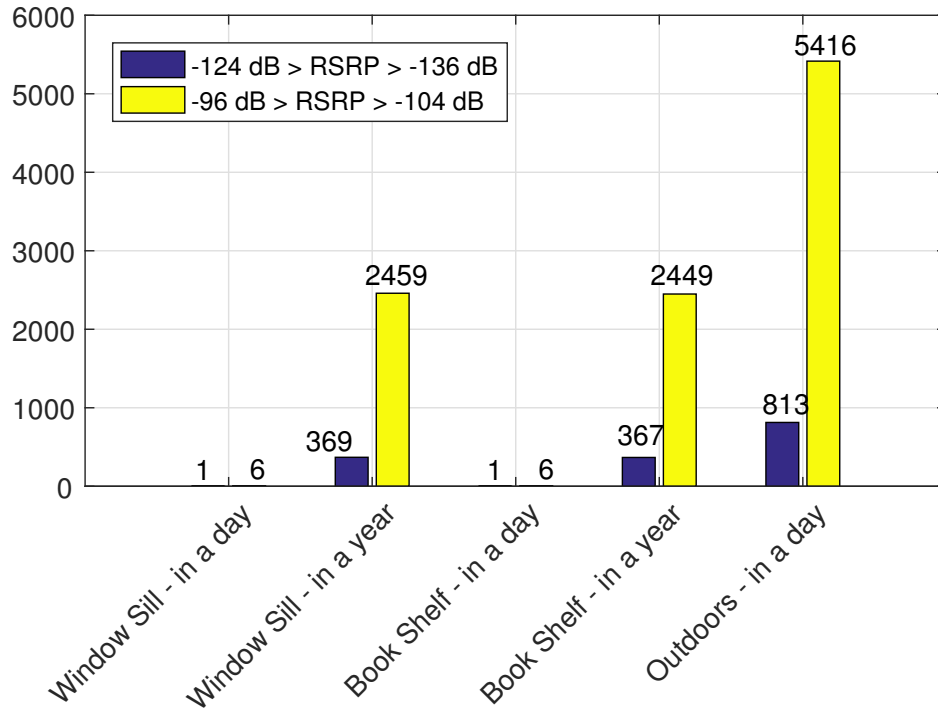


Figure 3.9: The gain represented in terms of additional packets that can be send

2. *Ambient energy availability*: The energy harvesting opportunities depends on the physical placement and mobility of the devices. Furthermore, even in a static deployment, the amount of energy that can be harvested varies spatially and temporally [26]. Several external factors may also determine the energy harvesting opportunities, such as room occupancy and weather in case of ambient light energy source.

3.3.2. CHALLENGES IN NB-IOT

In order to use energy-harvesting technologies effectively, a few challenges need to be addressed. The main cause for the challenges is the energy requirement by the NB-IoT UE devices. The power required for transmission and reception activities is high when compared to that obtained by the harvester. There is very little flexibility to scale down transmission power (determined by the eNB based on the coverage class) in the standards [38]. The following two tradeoffs must be dealt with.

1. *Coverage vs. energy*: As shown in Section 3.1.3, the device energy requirement is dependent on the payload transmission rate and the coverage class of the device. A poor radio link between the UE and the eNB results in high transaction time resulting in more energy consumption than in good coverage.
2. *Coverage vs. scalability*: The number of periodic reporting devices served is limited by the coverage class of the devices, as the devices in deep coverage consume the radio resources for a longer time.

Accounting for energy of device while performing link adaptation (determining the number of repetitions per physical channel and adapting MCS index based on the radio link, done by the eNB based

on the coverage class) in NB-IoT, optimizations on timer values such as the Active timer, the cDRX period, the Inactivity timer etc. to reduce time taken to reach PSM, can be adopted to reduce energy. Given the constraints and the tradeoffs, innovative solutions must be developed to make effective use of the harvested energy.

3.4. SUMMARY

In this Chapter, the energy characterization of an NB-IoT device in real-world settings is performed. The lifetime of the device is estimated under two different coverage conditions, for two reporting intervals. The significant difference between the estimations and the expected lifetime estimations are presented. It is shown that the device does not yet meet the lifetime requirements set in the standards. In order to increase the lifetime, this work investigates the possibility of harvesting energy from ambient sources. Three real-world data sets pertaining to ambient light in indoor and outdoor scenarios are analyzed. The gain in energy obtained is presented in terms of additional packets that can be served. The pressing challenges associated with energy-harvesting and those inherent to NB-IoT technology are presented.

4

ENERGY EXTENSION FRAMEWORK

This chapter introduces the xTEND framework. The two modules that form the framework, Energy- and Value- Aware Packet Scheduler (EVAPS) and Channel Aware Radio (ChAR), are described. The EVAPS module is mapped as a 0/1 incremental knapsack problem, and a lightweight threshold based solution to the problem is presented. The basis and the method of implementing the ChAR block are described.

4.1. MOTIVATION

As seen in the previous chapter, the NB-IoT UEs do not have a long lifetime, especially in deep coverage. While a bigger battery capacity is an option, it would only extend the battery lifetime at most by a few years. In order to achieve autonomy with respect to energy, we adopt ambient energy-harvesting techniques to augment the battery. A trivial solution is to just connect the harvester to recharge the battery and allow the node to have an added lifetime. However, the harvested energy is not uniform in time and space. Typical applications for NB-IoT have payloads of different priority and energy requirements. For instance, as mentioned in Chapter 1, with a parking sensor on a UE in the smart-parking use-case, the house-keeping data may have low priority, sensor data may have mid priority and an event (i.e., cars entering or leaving the zone) may have the highest priority. In such cases, the trivial solution will not give many benefits. Further, the payload size in each case may be different resulting in a difference in the energy requirements in each case. Therefore, a smarter energy management solution that considers both energy and priority of payloads in the decision to transmit a payload, subject to the spatiotemporal variations in harvesting energy, is required. Furthermore, energy efficiency must be maximized wherever possible, without modifying the NB-IoT network stack. While the stack and the protocol may offer several techniques to minimize energy consumption, such solutions cannot be adopted by an operator as such techniques need approval by 3GPP before being implemented in the field. Therefore solutions that are “out-of-the-box” that can be implemented with the current deployment and can serve an extensive set of use cases is required. The solutions must coexist in a deployment environment. Hence, in this work, a framework is proposed that binds solutions and can be ported on a sensor device deployed to serve applications.

4.2. DESIGN GOALS

This section details the design goals of the framework that binds the solutions required to maximize the utility of the device to the application while extending the device lifetime. The following design goals are set out for the framework:

1. The framework must extend the time to depletion and maximize the utility of the application it serves.
2. The framework must have the capability to be incoming energy aware.
3. The framework must cater to event-triggered applications (e.g., send payloads only when a car enters or leaves), periodic applications (e.g., only report the parking zone usage every hour) and applications that are both event-triggered and periodic (e.g., send payloads when event occur as well as house-keeping data periodically).
4. The framework should be light-weight and of low computational complexity.

In this work, all NB-IoT devices are considered to be statically deployed for the entire duration of their lifetime.

4.3. OVERVIEW OF THE xTEND FRAMEWORK

To meet the design goals set for the framework, in this thesis, the xTEND (eXtending the lifeTime through Energy-harvesting for NB-IoT Devices) framework is proposed. (See Figure 1.2). As shown in Figure 1.2, the framework has two main modules: the energy- and value-aware packet scheduler (EVAPS) module and the channel-aware radio (ChAR) module. The EVAPS deals with the decision problem of choosing the right payloads to transmit. In this work, every payload generated by the IoT application is considered to have a certain value associated with it. Therefore, xTEND deals with the decision problem of choosing to send a payload of a certain value. By maximizing the cumulative value, it is considered that the xTEND framework would have maximized the utility of the application. EVAPS can read the state of charge of the battery (available energy) and can take the input of energy prediction module as well. To make optimal decisions, EVAPS computes a transmission policy based on mapping solving the problem at hand to the 0/1 incremental knapsack problem. The transmission policy developed in EVAPS can handle any kind of traffic input (events and/or periodic payloads). The output of EVAPS is a decision of whether to transmit or drop (deferring is also possible) the current payload among a pre-defined horizon of payloads. If the decision is to transmit the payload, the second stage, employs a channel-aware radio.

The ChAR module identifies the coverage scenario by looking into the DCI information provided by the NB-IoT radio. The DCI information is provided by the NB-IoT chipset via serial communication in the debug port [14]. If the UE is in a coverage scenario where the number of subframe repetitions is minimum, the ChAR module does not play a role. However, if the UE is in deep coverage scenario, then ChAR amplifies the transmitted signal and tries to minimize the number of repetitions. This implies that the payload transaction can consume less time at the cost of a bit of extra power for amplification.

4.4. THE EVAPS MODULE

The energy- and value-aware packet scheduler (EVAPS) module deals with the scheduling of payload transactions in NB-IoT devices. This problem is formulated as a combinatorial optimization problem

such as the Knapsack problem. The 0/1 knapsack problem is a combinatorial maximization framework that deals with collecting items into a knapsack of fixed capacity. Each item is associated with a weight (subtracted from the capacity of the knapsack upon collection) and a value (that represents the reward for collecting that item). The problem deals with collecting items such that:

1. the sum of the weights, associated with each collected item, does not exceed the capacity of the knapsack
2. the sum of the values, associated with each collected item, is the maximum possible.

A finite horizon is defined which consists of the list of payloads (value-weight pairs), from the current payload, that forms the 'items' in the knapsack computation at that instant. The capacity of a knapsack translates to the capacity of the energy buffer. Since the device is equipped with an energy harvesting unit, the capacity of the energy buffer, and hence the knapsack, can increase as well [35]. Hence, the transmission policy translates into an incremental knapsack problem. An incremental knapsack problem, unlike the classical knapsack problem, does not have a fixed capacity [34]. The capacity increases over time.

Further, each payload is defined by a weight, corresponding to the energy required for its exchange, and a value, a reward obtained upon its successful exchange. If the weights, the values, and the knapsack increments are deterministic, the problem translates to a deterministic problem. In this work, the energy arrivals and payload arrivals are not known, however, the priority of the payloads (values) and its corresponding energy cost (weight) are predefined. This assumption is well within the limits of the use cases that apply to this technology. Given a set of payloads, the input to the EVAPS is the energy cost for payload exchanges, rewards obtained for the payload exchange, energy increments until the finite horizon if energy prediction is enabled, and the current battery state.

The target applications for NB-IoT devices can be characterized as such-

1. periodic applications: These applications consist of periodic payloads that are exchanged with a periodicity of δ , where $\delta \in \mathbb{R}^+$. A hyper period is defined as the least common multiple of δ and one day. The occurrence of the payloads is similar across the hyper periods. Within a hyper period (for instance a day), there are PD_c periodic payloads.
2. event-driven applications: These applications consist of payloads that are generated based on events/alarms. For the case of event applications, the hyper period is equal to one day. Within a hyper period, there are ED_c expected payloads.
3. periodic+event applications: These application consist of both periodic and event-driven payloads. The hyper period considered in this case is the least common multiple of δ and one day, where δ is the periodicity of the periodic payloads. Within a hyper period (for instance a day), there are $(PD_c + ED_c)$ payloads.

Let $i \in \mathbb{Z}^+$ denote the time instant; N_i represents the periodic payload to be sent at instance i and δ_{i+1} represent the period duration between the N_i^{th} and N_{i+1}^{th} payload. For periodic and periodic+event applications, the finite horizon ranges from δ_{i+1} until δ_{i+n} . For event-driven applications, the finite horizon is the same as the periodic application, with the period duration (δ) being equal to the hyper period. Among the $(n + 1)$ payloads, the framework chooses payloads that maximizes the total 'value', such that their total 'weight' is less than the 'knapsack capacity'. Once a decision is made, it is irrevocable. Upon optimization, only the decision to transmit the current payload is taken. The system implements a receding finite horizon and finds the local maxima in each finite horizon. Hence, on

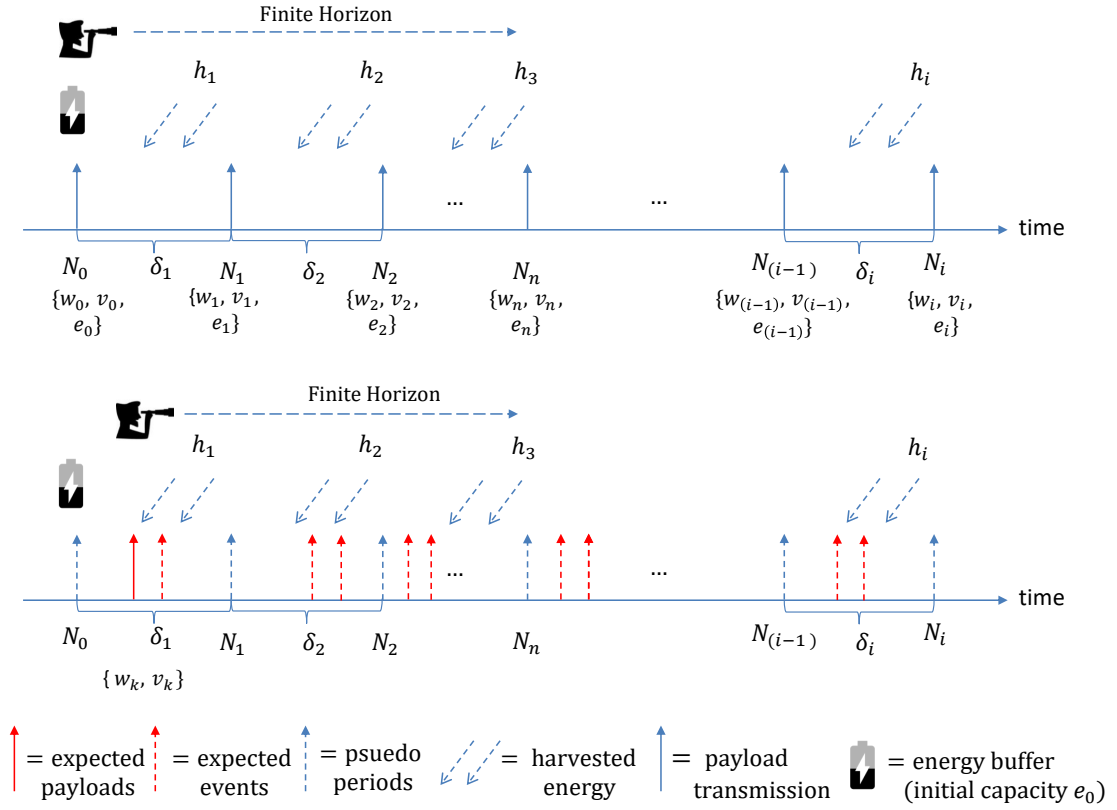


Figure 4.1: Payloads in periodic (row 1) and event-triggered applications (row 2)

arrival of the next payload, the knapsack computation for n payloads from the current payload is performed. The receding horizon helps reduce the errors in energy prediction and the computation of energy cost of a payload.

Before the incremental knapsack problem is formulated, the weights and values for a payload are described:

- **a weight (w_k) \iff energy per payload**

The weight corresponds to the energy consumption cost of exchanging a payload for a stationary NB-IoT device, given a radio condition. Since the applications considered are immobile, it can be assumed that the energy consumption cost for a payload does not vary. Hence, all the weights in a finite horizon of a given payload size are the same as that for the current payload. The weight w_k is defined as a positive integer multiple of the energy units required for payload k to be transmitted. The energy unit U_e is calculated as the least common multiple of the energy costs of all the payloads in the finite horizon.

- **a value (v_k) \iff priority of payload**

The value is defined as per the requirement of the application. This variable provides a dimension for the application to estimate and distinguish utility of different payloads. A value function may be defined as a function of time or statically defined. For instance, for the smart parking

use-case, a value function may be defined based on the time of a day, as

$$v_i = \begin{cases} v_1, & 7:00 - 9:00, \text{ and } 16:00 - 18:30 \\ v_2, & 9:00 - 16:00 \\ v_3, & \text{otherwise} \end{cases}$$

where $\forall v_i \in \mathbb{Z}^+$.

If e_i represents the capacity at the i^{th} instance, between any two time instances i and $(i + 1)$, the capacity $e_{(i+1)} \geq e_i$, if no selections are made.

Further,

- If the initial energy stored in the buffer is e_0 and the maximum allowed is e_{\max} ,
- the leakage associated with the buffer is σ ,
- the energy harvested between the two consecutive instances $(i - 1)$ and i is h_i ,

then the energy estimated/capacity at the i^{th} instance is:

$$e_{i+1} = e_i + h_{i+1} - w_i x_i U_e - \sum_{j=0}^{ED_c-1} w_j y_j - \sigma \quad (4.1)$$

For applications with periodic payloads, a selection of the payload N_i is performed as x_i and for applications with event payloads, given there are ED_c expected events in an hyper period, a event payload is selected as y_j , where x_i and y_j are 1 if selected to transmit or 0 otherwise.

At any instant of payload arrival, the decision to transmit a payload is based on a maximization problem. The objective function to maximize:

$$\text{Max} \sum_{i=0}^n \sum_{j=1}^{ED_c-1} v_i x_i + v_j y_j \quad (4.2)$$

subject to the constraint:

$$\sum_{i=0}^n \sum_{j=0}^{ED_c-1} (w_i x_i + w_j y_j) \leq e_i \quad (4.3)$$

The above equations apply for periodic applications (with $w_j = 0$, $y_j = 0$), event triggered applications (with $w_i = 0$, $x_i = 0$) and periodic+event triggered applications.

SOLVING THE INCREMENTAL KNAPSACK PROBLEM

The algorithm adopted in EVAPS is presented in Algorithm 1. Algorithm 1 draws from the dynamic programming solution to classical knapsack problem [39], and adds an innovative approach to extend the solution to incremental knapsack problem with a single item at each time step. This is done so as to make the module capable of predicting the harvested energy. If the prediction is not done, then it suffices to solve using the classical dynamic programming solution.

The traditional dynamic programming solution involves building a table of size $n \times M$, where n is the total number of items in the finite horizon and M is the total number of packets that can be served

at an instant and is defined as $\frac{e_{\max}}{U_e}$. The solution identifies the maximum value among all combinations of items in the corner cell (table[n][W]) of the table. The approach has a time complexity of $O(n.M)$. The modified solution fills the table in the same way as the traditional solution (*Populate_table_DP()*) [39]. The difference occurs with the incoming energy at a time instance i . Whenever the device receives ' q ' number of U_e units of energy, the solution increments the current column count W with ' q ' additional columns to the table, backtracks to the previous rows and copies the last filled value in that row to each additional column, enforcing the causal constraints of the incoming energy (lines 6-14). Figure 4.2 represents this when $q = 1$. If the incoming energy is a fraction of U_e , then the column count remains the same and the energy is added to the incoming energy at the next instance. The increment in the current capacity W at each time step i is determined by the energy prediction block, *energy_prediction(i)*, in Algorithm 1. The maximum value is obtained in the corner cell (table[n][W]). Compared to the traditional solution, Algorithm 1 carries an additional complexity of backtracking to all the previous rows, once during each row increment. To identify the items contributing to the maximum value backtracking is performed in the table, as in the traditional solution [39] (*Identify_items_DP()*), and the items are identified.

Algorithm 1 Solving incremental knapsack problem

Require: Array of Weights: $w[]$, Array of Values: $v[]$, Current Capacity: W , Maximum Capacity: M , Total number of items: n

```

1: function INCREMENTALKNAPSACK( $w[], v[], W, M, n$ )
2:   table[row][col]  $\leftarrow 0$  for all row = 0,...n and col = 0,...M
3:   for row  $\leftarrow 0$  to  $n$  do
4:     for col  $\leftarrow 0$  to  $W$  do
5:       Execute: Populate_table_DP(w,v)
6:       if row  $\geq 2$  and col == 0 then
7:         temp  $\leftarrow W$ 
8:          $W \leftarrow W + \text{energy\_prediction}(i)$ 
9:         for  $a \leftarrow \text{row}$  to 0 do
10:          for  $b \leftarrow C$  to temp do
11:            table[ $a-1$ ][ $b$ ] = table[ $a-1$ ][temp]
12:          end for
13:        end for
14:      end if
15:    end for
16:  end for
17:  Execute: Identify_items_DP()
18:  return decision for first item
19: end function

```

With this method, solving the knapsack problem at each payload arrival would require a massive amount of computations, especially with a large finite horizon, and would itself prove to be an energy overhead for the device. However, since the weights and values are known beforehand, the computations can be performed offline and the decision to transmit/drop (defer) can be stored in a Lookup Table (LUT). The rows of the table represent the capacity from e_{\max} to 0 with a total of ' M ' ($\frac{e_{\max}}{U_e}$) number of rows. Each column represents payloads (for periodic applications) or combination of payloads (for event triggered and periodic+event applications) among the list of available payloads. The content in each row-column pair consists of a decision to transmit or drop (defer), given a payload (column) and the available energy capacity (row). At each instance of a payload arrival, the device looks up at the corresponding row-column pair (current capacity-current payload) and identifies the decision. In the case of a periodic application, the number of columns is limited to the number of periodic payloads in a hyper period. For event-triggered applications and periodic+event applications, since the arrival of events are not known beforehand, the events that have occurred in a hyper period can be tracked by forming all possible combinations of events due to occur in the hyper period when an event occurs. Hence, the number of columns is a function of a combination of events that may occur in the hyper period once a payload has arrived. The number of columns for event-triggered

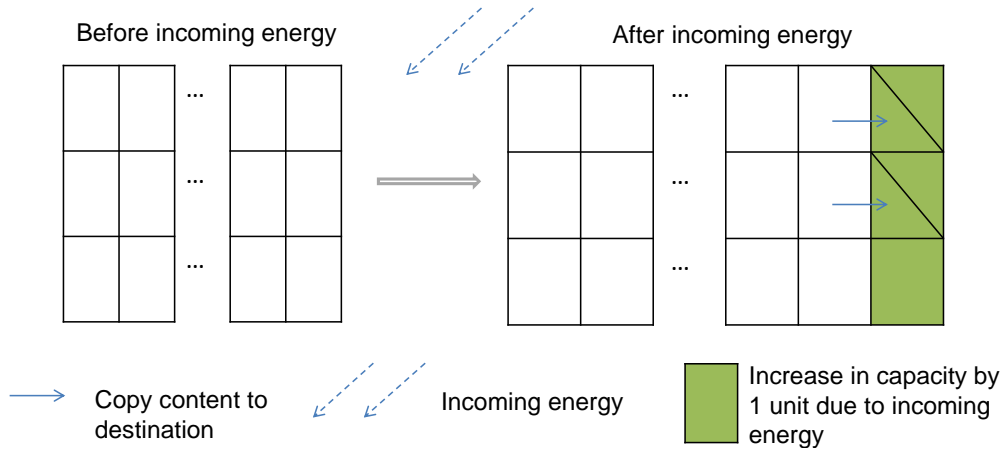


Figure 4.2: The formation of the table structure as part of the dynamic programming solution to solve the incremental knapsack problem

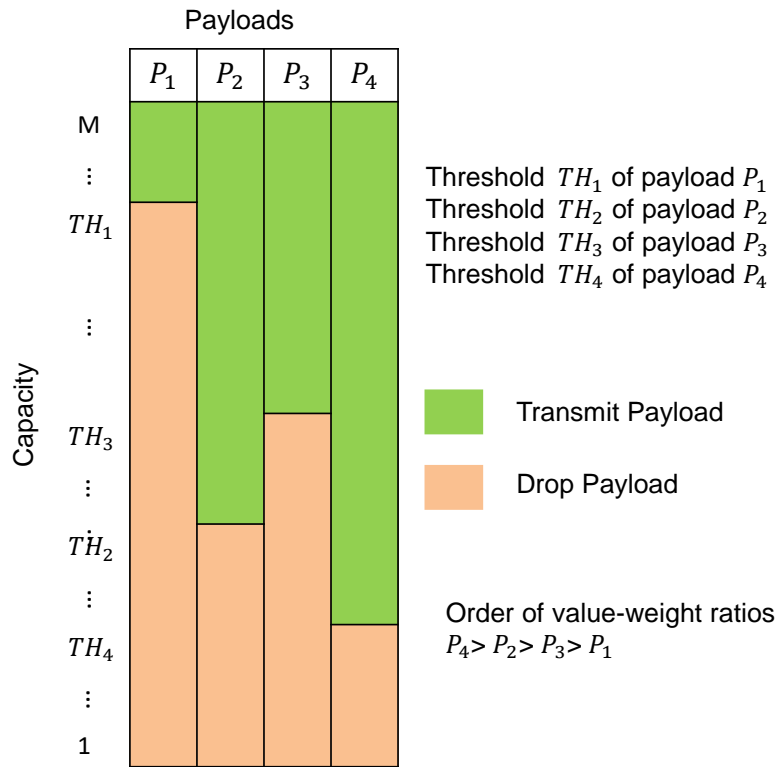


Figure 4.3: Representation of the lookup table with four payloads and their capacity thresholds

applications and for periodic+event triggered applications is obtained as such, respectively:

$$ED_c \times 2^{ED_c-1} \tag{4.4}$$

$$(ED_c \times 2^{ED_c-1} + 1) \times PD_c \tag{4.5}$$

where PD_c represent the number of period payloads and ED_c represent the number of event payloads.

A threshold structure forms in the lookup table for a particular set of value-weight pairs. A threshold structure in the lookup table implies that for each payload, beyond its threshold (in the subsequent rows) in the lookup table, the decision is always to drop the payload. The threshold structure for a lookup table with four payloads is represented in Figure 4.3. Forming a threshold structure would reduce the memory requirements for storing a table, the energy requirement for accessing the memory and the initial effort to set up the lookup table. Further, this would also enable to modify the value-weight pairs and the finite horizon online without the massive amounts of computations required to form the table. This provides energy savings and flexibility in operations.

Finding 1. Given a number of payloads identified by their value-weight pairs $(v_k, w_k), \forall k \in \{1, 2, \dots, P_N\}$, a threshold structure exists for the value-weight pairs when

1. an increment to weight w_l from the smallest possible weight 1, in a value-weight pair (v_l, w_l) , results in a value-weight ratio less than the ratio formed by the smallest value and its weight. That is, $\frac{v_l}{w_l} < \frac{v_s}{w_s}$ where (v_s, w_s) is a value-weight pair such that $v_s = \min(v_k) \forall k$.
2. the weight, w_k , must be greater than or equal to twice the weight of any pair whose ratio is greater than (v_k, w_k) , and its value is lesser than v_k . That is, $w_k \geq 2w_l \forall l \ni \frac{v_k}{w_k} \leq \frac{v_l}{w_l}$ and $v_k > v_l$.

Finding 2. The threshold for a payload p , having a value-weight pair (v_p, w_p) , can be computed using the following equation.

$$Threshold_p = \begin{cases} \frac{F_H}{P_N} O_p + \frac{F_H}{P_N} \sum_{m=0}^{O_p-1} AW_m + \kappa, & \text{if } O_p \geq 1 \\ AW_{O_p}, & \text{if } O_p = 0 \end{cases} \quad (4.6)$$

where κ is defined as:

$$\kappa = \begin{cases} AW_{O_p}, & val(O_p) < val(O_p - 1) \\ AW_{O_p-1} + (weight(O_p) - 2weight(O_p - 1)), & val(O_p) > val(O_p - 1) \end{cases}$$

In the above equation, F_H is the finite horizon, P_N is the number of distinct value-weight pairs. If all value-weight pairs are sorted in descending order based on the values, and each pair is indexed starting with 0 (i.e., the highest value and its corresponding weight is index 0, the next highest value and its corresponding weight is index 1 and so on), then O_p is the index of the value-weight pair (v_p, w_p) in this sorted list of pairs. AW_{O_p} is the additional weight of a payload p indexed by O_p , which is defined as the ratio between the difference of energy consumed by p and the unit energy, to the unit energy, i.e., $\frac{Energy(p) - U_e}{U_e}$. $val(O_p)$ is the value and $weight(O_p)$ is the weight of a payload p indexed by O_p . The F_H is chosen such that it is a multiple of P_N .

Lemma 1. A threshold structure exists for a 0/1 knapsack problem when the value-weight pairs are chosen according to Finding 1, and the threshold for a payload can be computed using Equation 4.6.

Proof. The proof of this statement is split into two parts: first part to prove a threshold structure indeed exists when the stated conditions are satisfied, and the second part to show that the threshold can be computed using the equation.

Proof for threshold structure existence. Given a finite horizon F_H , and the list of value-weight pairs in the horizon, the policy would accumulate values as according to the 0/1 knapsack problem. If the capacity is less than the sum of the weights of all the items in the horizon, then the policy drops the low value payloads, i.e., the capacity is just enough to accumulate all the higher value payloads. When the weights of the pairs are random, then a definite threshold need not exist, as the solution to knapsack performs a combinatorial maximization.

A sufficiently large difference among weights will ensure that after a certain capacity a lower value-weight payload will not be selected anymore in the optimal combination of item selection. This is enforced by the condition 2 of Finding 1, wherein the weight w_k of any payload p_k must be greater than twice the weight of any pair (v_l, w_l) whose ratio is greater than (v_k, w_k) and the value v_k is greater than $v_l, \forall l \ni \frac{v_k}{w_k} \leq \frac{v_l}{w_l}$. In this case, in a F_H , the combination that would involve the payload p_k is only when all the payloads p_l are involved, as the larger ratio payloads p_l have a weight less than or equal to half of the item's weight. Adding the low value-weight pair p_k costs at least twice as adding the high value-weight pair p_l , and hence the policy chooses all the high value-weight ratios p_l in the finite horizon till the capacity permits. If the capacity remains, the low value-weight pair p_k is chosen. If the ratio of weights w_k and w_l of the payloads p_k and p_l is between 1 and 2, then a combinatorial optimization results in the choice of the payload depending on the available capacity. By enforcing the ratio to be greater than or equal to 2, the optimum choice is always to choose the higher value-weight ratio with any available capacity.

Since the values are relative to each other, only the order of the values matters rather than the numerical value. If the weight of a certain payload is to be increased while guaranteeing a threshold structure, then the increment of the weight must ensure that value-weight pair has a value-weight ratio less than the ratio formed by the smallest value and its weight. This condition eliminates the occurrence of a scenario where two payloads (v_k, w_k) and (v_l, w_l) have their value-weight ratio as $\frac{v_k}{w_k} \leq \frac{v_l}{w_l}$, and have relation $v_k < v_l$ and $w_k < w_l$, which does not result in a threshold structure. The choice of the payload depends on the availability of the capacity.

Proof for threshold computation. The trivial case for 0/1 knapsack is when all the weights are equal. In this case, the optimal solution is achieved by sorting the payloads by their values in descending order and selecting the items until the capacity is filled. It should also be noted that there is a threshold structure in this trivial case for varying capacity, which can be computed using $\frac{F_H}{P_N} O_p$. If the weights are different, then the additional weights of all the payloads must be considered. Since the weights are chosen in such a way the higher value payloads are chosen first, it is guaranteed that all items up to $O_p - 1$ will be included if O_p is also going to be included. Therefore, the summation of additional weights of all the high value-weight ratio pairs is considered of which the fraction of F_H and P_N gives the threshold when $O_p \geq 1$. Further, the additional weight of the payload considered is obtained through κ . If the value of the payload p is less than the value of the payload that has the value-weight ratio immediately greater than the ratio of p , i.e. $val(O_p) < val(O_p - 1)$, then the threshold increases by the additional weight of the current payload. If the value of p is greater than the value of the payload with index $O_p - 1$ i.e. $val(O_p) > val(O_p - 1)$, the weight of the payload p is greater than or equal to twice the weight of the payload $O_p - 1$, by condition 2 of Finding 1. The contribution to the threshold when the payload p has a weight equal to $weight(O_p - 1)$, is the same as AW_{O_p-1} . The threshold is not formed when the ratio of the weights, $weight(O_p)$ to $weight(O_p - 1)$, is between 1 and 2. The payload p contributes to the threshold with additional weight from ' $2weight(O_p - 1)$ '. Hence the additional weight contribution from the payload p is $AW_{O_p-1} + (weight(O_p) - 2weight(O_p - 1))$.

A trivial case is when $O_p = 0$, which means we are dealing with the highest value payload only. In this case, the threshold will be the additional weight of the payload, i.e., select the item if there is sufficient capacity left. \square

4.5. THE CHANNEL-AWARE RADIO MODULE

The energy consumed by the NB-IoT device is determined by the power and time taken for the payload exchanges. For NPUSCH, when the number of repetitions for the physical channel in uplink is greater than 2, the serving cell configures the device to transmit at P_{\max} (23dBm). If the number of repetitions

is either 1 or 2, then the power control is performed by the following equation [3]:

$$P_{\text{NPUSCH}} = \min\{P_{\text{max}}, 10\log_{10}(M) + P_{\text{target}} + \alpha L\} \text{dBm}$$

where

- M - a constant depending on NPUSCH tone configuration,
- P_{target} - targeted received power level at eNB,
- α - path loss adjustment factor and
- L - estimated path loss.

The coverage enhancement techniques increase the transaction time of a device, thus depleting the energy buffer. The repetitions and the MCS (Modulation and Coding Scheme) is determined by the intelligence at the network, based on channel estimations. By reducing the repetitions, the transactions finish faster and the device spends less time in transmission/reception activities. In this work, a channel aware radio is proposed which is used when EVAPS schedules a payload for transmission. The ChAR block makes use of the 2 dBm tolerance allowed from the maximum configured transmission power of 23 dBm [40]. The channel conditions are identified based on the DCI message logs that can be obtained from the serial port of the NB-IoT chipset. The DCI messages (DCI-N0 and DCI-N1) contain information about the repetition number of the transport blocks in the uplink (DCI-N0 block)/downlink channel (if DCI-N1 block) and the repetition number of the NPDCCH channel that carries the DCI. If the repetition number of the transport block in the uplink is greater than 2, then the ChAR module is used. A screenshot of the DCI message that indicates the repetition numbers is shown in Figure 4.4.

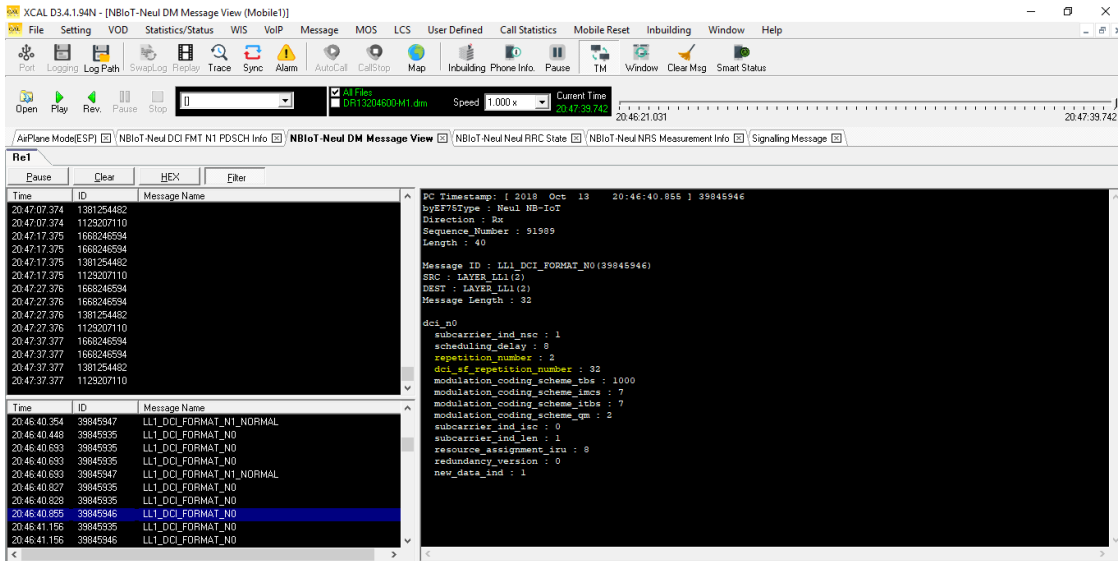


Figure 4.4: Screenshot of the DCI message log analyzed on the Accuver XCAL tool. The repetition numbers are highlighted.

As device identifies the number of repetitions in the uplink to be greater than 2, the ChAR module is activated and increases the transmission power of the device from the maximum allowed transmission power of 23 dBm (P_{max}) to the regulation limit of 2 dB. By making use of the 2 dBm slack when required, the number of repetitions reduces without losing coverage. The device remains in the transaction for a lesser amount of time and releases the radio resources it occupied faster. Hence, with the

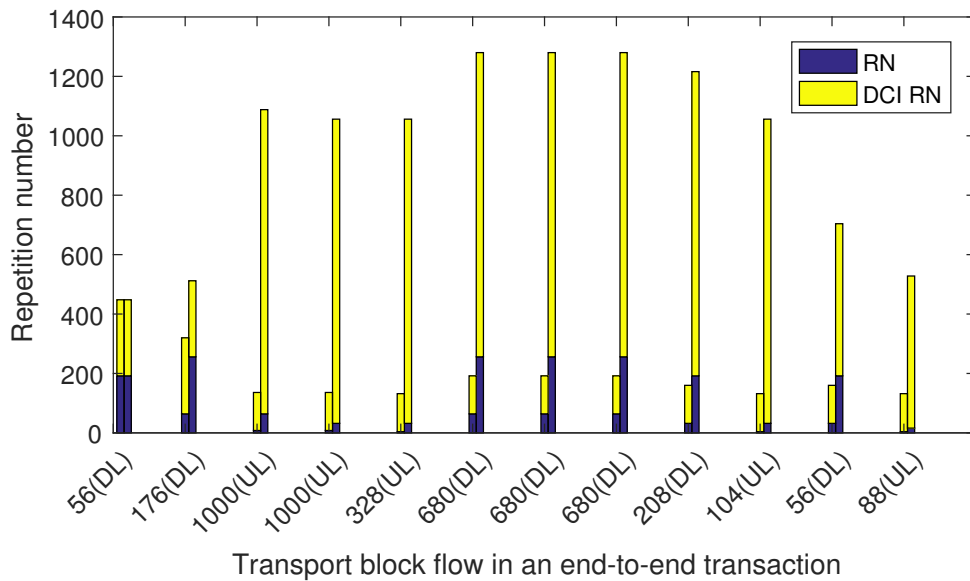


Figure 4.5: The Repetition count for NPUSCH (UL RN), NPDSCH(DL RN), and NPDCCH (DCI RN) subframes of a 200 bytes payload in both uplink and downlink, with (left bars) and without (right bars) the additional gain

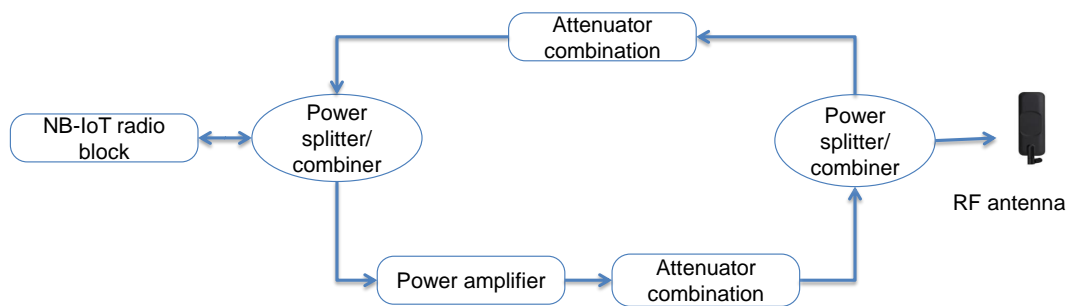


Figure 4.6: The block diagram to implement ChAR block to NB-IoT radio modem for analysis.

ChAR block, a two-fold benefit is obtained: in device energy savings and time savings in the physical channels. To benefit in device energy consumption, the reduction in the number of repetitions should be less than the factor by which the transmission power level is increased. Figure 4.5, shows the repetition counts of the transport block in the NPUSCH (UL RN), NPDSCH (DL RN), and the NPDCCH channels (DCI RN), with and without the additional gain in transmission. The figure indicates a reduction in the repetition counts with the increase in the transmission power.

The channel awareness is crucial, even in use case scenarios where the devices are immobile. The channel conditions need not be static such as when a vehicle blocks the sensor device in a smart parking scenario.

Since the power amplifier used is embedded into the NB-IoT chipset, and there is no access to it, an external power amplifier is used. Figure 1.2 shows the block diagram to implement the ChAR for analysis. The antenna output from the NB-IoT module is split into two paths, using a power splitter/-combiner, one with the power amplifier and an attenuator combination to obtain the desired gain of 1 dB/2 dB, and the other path acts as the receiver chain. The two paths are combined and connected to an RF antenna, using the power splitter/com-

biner at the RF antenna was verified to be amplified using a spectrum analyzer. The variable gain is obtained with the help of combinations of RF attenuators.

4.6. SUMMARY

In this chapter, a framework is proposed that performs intelligent energy management techniques. The framework consists of two modules - EVAPS and ChAR. Each payload is defined by a value, and the EVAPS module makes intelligent decisions based on the current energy capacity, the energy required for the packet and the value of the packet. The packet is either decided to be transmitted or dropped (also deferred). The module is mapped as a 0/1 knapsack problem, and a threshold based scheme is identified. The ChAR module, based on the channel conditions, boosts the transmission power to the tolerance level limit. This reduces the effect of the coverage enhancement techniques on the energy consumption of the device, without losing out on the coverage.

5

PERFORMANCE EVALUATION

In this chapter, the xTEND framework is analyzed in two stages. In the first stage, the EVAPS module is evaluated against an existing solution and an offline clairvoyant algorithm, for three types of applications: periodic, event-driven and periodic+event applications. In the second stage, the ChAR block is analyzed for an additional gain step of 1 dB. To evaluate the performance of the proposed framework, a smart parking use case is considered.

5.1. SMART PARKING USE-CASE

A typical use case for NB-IoT enabled devices is a smart parking environment. A smart parking scenario involves sensor devices deployed to identify available parking options, and real-time notification of all updates. Further, sensor devices that serve other functionalities such as air quality or temperature monitoring systems can also be a part of this environment. Many pilot smart parking systems that use NB-IoT have been reported in different parts of the world [41–44]. The improved connectivity range for devices, the 10+ years device lifetime and assured quality of service of the licensed spectrum are factors that have played a role in the adoption of the technology for the use case.

The use case comprises of sensors that can be primarily grouped as periodic sensors, event-triggered sensors, or a sensor device that has a combination of the both. Typical examples of periodic messages would be air quality measurements, temperature measurements, or status update messages etc. The car arrivals, alarm messages would be event triggered. Further, the device could have a combination of sensors that detect, for instance, the arrival of cars, and also reports the sensor health status after a fixed duration. Hence, it becomes essential for the framework proposed in Chapter 4 to be applicable in all such scenarios.

5.2. SYSTEM EVALUATION

In this section, the xTEND framework is evaluated under different conditions. The EVAPS and the ChAR module are evaluated separately as the two modules function independently to each other.

5.2.1. EVALUATION SCENARIO

EVAPS

The EVAPS module is compared against the offline clairvoyant algorithm (CA) and a jumping threshold (JT) based solution in the literature [35]. The clairvoyant algorithm has complete knowledge of the incoming energy for the entire evaluation period, and hence form the most optimal and informed scheduling decision. The jumping threshold based solution is an online threshold based scheme. Given definite bounds on the value-weight ratios, the algorithm forms a threshold for the value-weight ratio based on an instantaneous threshold. The instantaneous threshold is a function of capacity left at any instant. Unlike the EVAPS module which has a linear threshold model, the thresholds of the JT vary exponentially. However, given a bound on the value-weight ratios and a capacity value, the thresholds are fixed. In EVAPS, the thresholds are also a function of the finite horizon, a parameter that can be determined by the operator.

The evaluation of the EVAPS module is performed for periodic, event-driven and periodic+event applications. In each application scenario, the payloads are characterized by their weight and their value. In a smart parking scenario, an example value distribution of the payloads can be based on the time duration in a hyper period. For instance, if the hyper period is defined to be a single day, then a value distribution of the payloads can be determined as such:

$$v_i = \begin{cases} v_1, & 12:00 - 6:00 \\ v_2, & 6:00 - 12:00 \\ v_3, & 12:00 - 18:00 \\ v_4, & 18:00 - 12:00 \end{cases} \quad (5.1)$$

where $\forall v_i \in \mathbb{Z}_+$.

The value function identifies four different values for the payloads that occur in a day. Further, the weights of the payloads are determined based on the energy consumption cost of the payload transaction. If all the payloads cost the same amount of energy, then the weights of all the payloads are the same. However, the energy consumption cost of the payloads can vary based on the size of the payload. In such scenarios, the payloads can have a different weight distribution. Hence, in the case of periodic and event-driven applications, two kinds of value-weight distributions are evaluated: payloads of the same type (payloads have the same weight but different values) and payloads of different types (payloads have different weights and different values). In evaluation of same type messages, the values and weights considered are: $v_k = [6,7,8,9]$, $w_k = [1,1,1,1]$. In evaluation of different type messages, the values and weights considered are: $v_k = [24,32,36,43]$ and $w_k = [2,8,4,1]$. The value-weight pairs are identified based on Finding 1 presented in Chapter 4. The values identified are attributed to the payloads as per the value function described in equation 5.1. In the analysis, each application is supplemented by ambient energy harvesters. For the evaluation, this work considers a real-life indoor ambient light harvesting dataset [36] (the *bookshelf* dataset) presented in Chapter 3. The dataset reflects the harvesting scenario in indoor conditions and hence can be compared to the underground/indoor smart parking systems. Further, evaluation is only performed for the indoor ambient energy dataset, due to the low amount of incoming energy in this case. The case of outdoor ambient energy harvesting is not evaluated due to the availability of a considerable amount of incoming energy, as presented in Chapter 3. In each of the application, the energy consumption of a 130 byte payload transmission with 12 bytes of acknowledgment reception, presented in Chapter 3, is used in the analysis. The initial capacity of the battery is considered to be 5 Wh.

CHAR

The CHAR block is evaluated in a coverage condition where $RSRP$ ranges from $-118 \text{ dB} > RSRP > -136 \text{ dB}$, with 1 dB additional gain step.

5.2.2. EVAPS EVALUATION

In this section, the system evaluation is performed and comparisons are drawn with the CA and the JT algorithms. The evaluation is performed for all three types of applications.

Periodic applications

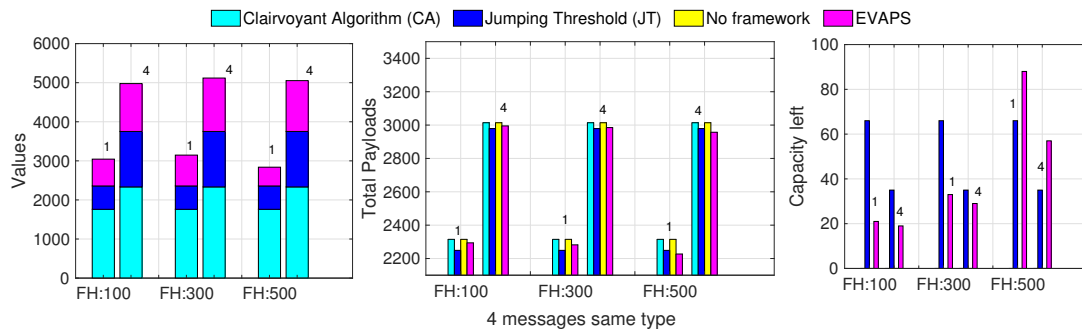


Figure 5.1: Periodic application serving 4 payloads of the same type. Additional value accumulated with respect to no framework scenario (left), the total number of payloads scheduled (center) and the capacity left at the end of the evaluation period (right) with varying finite horizon and evaluation periods for the schemes considered

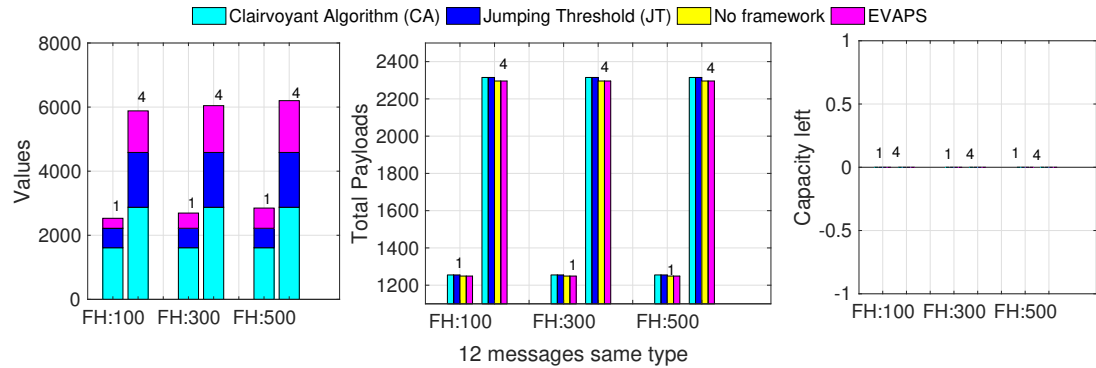


Figure 5.2: Periodic application serving 12 payloads of the same type. Additional value accumulated with respect to no framework scenario (left), the total number of payloads scheduled (center) and the capacity left at the end of the evaluation period (right) with varying finite horizon and evaluation periods for the schemes considered.

In a smart parking scenario, certain messages/updates would be periodic in nature. For instance, the health status of the sensor device, the battery status of the device etc. The payloads, categorized as same type (same weights) and of different types (different weights or values), as presented in Section 5.2.1, are used in the evaluation. The problem of the same weight and same values translate to the behavior of the device without any framework. In the analysis, the payload arrivals for two different kinds of periods are analyzed - one payload every 6 hours and one payload every 2 hours. In the case of a periodic reporting interval of once every 6 hours, there are 4 distinct valued payloads. Hence, the periodic rate fit within the minimum rate required by the value function described in Section 5.2.1. With the periodic reporting interval of 2 hours, each distinct value is attributed to 3 payloads. Further,

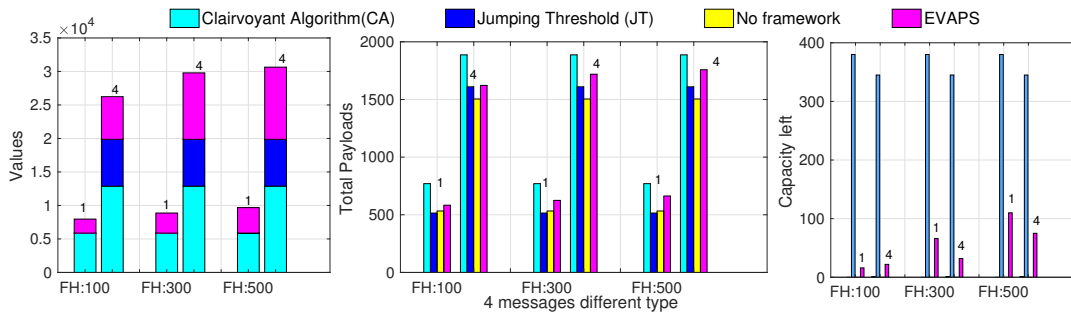


Figure 5.3: Periodic application serving 4 payloads of different type. Additional value accumulated with respect to no framework scenario (left), the total number of payloads scheduled (center) and the capacity left at the end of the evaluation period (right) with varying finite horizon and evaluation periods for the schemes considered.

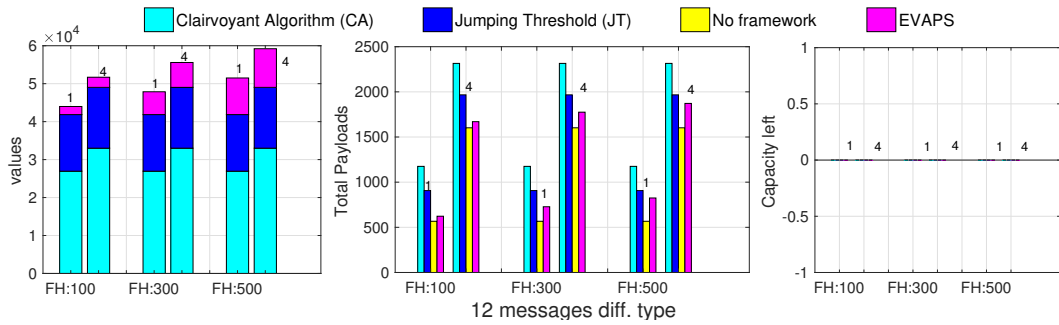


Figure 5.4: Periodic application serving 12 payloads of different type. Additional value accumulated with respect to no framework scenario (left), the total number of payloads scheduled (center) and the capacity left at the end of the evaluation period (right) with varying finite horizon and evaluation periods for the schemes considered.

two evaluation periods are considered in each case - 1 year and 4 years. This is a sufficient enough duration for the device to reach first complete depletion of its capacity.

The performance analysis is carried out with varying parameters such as the finite horizon, the duration of analysis and the periodicity between payloads. The values accumulated, the number of payloads transmitted and the capacity left at the end of an evaluation period are the metrics for comparison among the three schemes. Figures 5.1, 5.2, 5.3 and 5.4, presents the results of the evaluation. Each figure presents the three metrics: the additional accumulated value with respect to the 'No framework' scenario (left), the total number of scheduled payloads (center) and the total capacity left at the end of the evaluation period (right). The variation in these metrics with the varying finite horizon and evaluation periods are depicted in the figures. The evaluation period (in years) is shown on top of the bars in the figures. Following observations can be drawn from the figures:

- As per threshold equation 4.6 of Finding 2, presented in Chapter 4, increase in the finite horizon increases the threshold value. The threshold of the low value-weight ratio payloads become closer to the total available capacity with an increase in the finite horizon. This implies that the low value-weight ratio payloads are dropped early, conserving the capacity for the higher ratios. For short evaluation periods (1 year) that has less number of payloads, with increasing finite horizon, the value accumulated by EVAPS decreases after a certain horizon as the large threshold defers the low priority payloads. However, this is reflected in the decrease in the corresponding 'number of payloads' and an increase in the 'capacity left', as the framework becomes more conservative. This can be identified from Figure 5.1. The collected value increases as more high value-weight ratio payloads are chosen.

- The effect of increasing finite horizon is reflected more in payloads of the different type, as the low value-weight ratio pairs have a weight equal to or greater than or equal to twice the weight of the higher value-weight ratios. Hence dropping the low value-weight ratios conserves the capacity for the high value-weight ratio payloads.
- With the increase in the periodicity of messages there are more payloads to be served in an evaluation period. In the analysis, the values are distributed equally among the payloads. This implies that there are more low value-weight ratio payloads in comparison to a case with less periodicity, in a given evaluation period. With a large F_H ($=500$), the threshold for low valued messages is increased, and the capacity is conserved for the high valued messages.
- In the case of different type of messages with a smaller F_H , more of the low value-weight pairs are accumulated. This, in turn, depletes the capacity faster. However, with a larger F_H , the capacity is conserved for the higher value-weight ratio pairs, thus increasing the total value collected. This is also reflected in the increase in the capacity left and in the number of payloads, with increasing F_H .
- The choice of the finite horizon is dependent on the evaluation period. For the device to maximize the values accumulated over a long period irrespective of the type of the message or the periodicity, a large finite horizon is required.

Event-driven applications

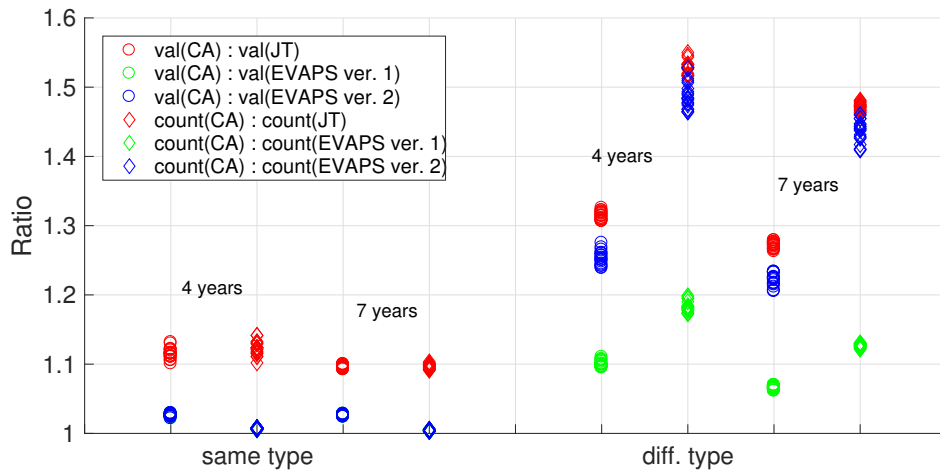


Figure 5.5: Only events scenario: ratios of values accumulated, number of payloads scheduled by the clairvoyant algorithm to that of EVAPS ver. 1, EVAPS ver. 2 and Jumping threshold. The functions `val()` and `count()` returns the total value accumulated and the number of payloads scheduled.

Smart parking scenarios benefit from event-driven applications by the context. A realistic application scenario may be outlined by alerts, such as the arrival of vehicles in parking spots, and alarm events, namely to be driven in case of fire or emergency. These applications are generally stochastic in nature. Since the weight and value of the messages are known beforehand, by defining the possible payloads as per finding 1 and their expected number of arrivals, a lookup table with a threshold structure can be constructed.

Two versions of EVAPS are evaluated in this case. In version 1, the framework keeps track of the events that have occurred in a hyper period. Hence, the lookup table (LUT) consists of an additional number of columns, where each column consists of a horizon with the available payloads in the hyper period

up to the last payload in the horizon. However, the size of the LUT increases exponentially with the rise in events.

Hence, in version 2 the events that have occurred in a hyper period is not tracked. This reduces the size of the LUT with a loss in the value accumulated. As with the periodic payload application case, EVAPS is compared with the clairvoyant algorithm and the jumping threshold solution. For a fixed finite horizon and two evaluation periods, the events in a hyper period occur randomly. In the evaluation, for each distribution, at least 20 trials with random generation of events are performed. In each case, up to 4 events can occur in a random order in a hyper period. The hyper period is 1 day, which reflects real-world scenarios. The two types of value weight pair distribution used in the evaluation of the periodic case are also considered here. A finite horizon $F_H = 40$ is chosen for the framework. The choice of a relatively small F_H is justified by the sparse occurrences of events in a hyper period. Two evaluation periods are considered in both the cases - 4 years and 7 years. This is a sufficient enough duration for the device to reach first complete depletion of its capacity. Figure 5.5 depicts the ratio of value accumulated by the clairvoyant algorithm to the jumping threshold, the EVAPS ver. 1 and EVAPS ver. 2. Following are the observations from the evaluation:

- All the three schemes perform closer to the global optimum, for the same type of messages. This due to a tight bound on the value-weight ratio considered. The difference in collecting a low and high value-weight ratio is not very significant. As the bound on the value-weight ratio increases, this difference increases, and the performance decreases.
- Over the evaluation periods, the ratios move closer to one. The given harvesting profile determines the energy increments and the rate of increment in the capacity. If the rate of increments are less and the available capacity is less than the threshold values of the low value-weight ratios, the messages are dropped and only the high value-weight ratio pairs are chosen, as the clairvoyant algorithm.
- The difference between the ratios $\text{count(CA)} : \text{count(EVAPS ver.1)}$ and $\text{count(CA)} : \text{count(EVAPS ver.2)}$ varies significantly in the same type and different type payload scenarios. So is the case with the ratio of values in both cases. However, this difference does not exist when the weights are the same. When the payloads have different weights, it benefits to keep track of the occurred events in a hyper period.

Periodic+event applications The framework is evaluated with periodic and event-triggered payloads. Four same type events with values $v_k = [6,7,8,9]$ and weights equal to 1 randomly occurs along with a periodic triggered payload of value = 5 and weight = 1. Figure 5.6 represents the ratio of value accumulated by the clairvoyant algorithm to the other two schemes. The F_H considered is equal to 40, and two evaluation periods of 4 years and 7 years are considered. Following are the observations for this scenario:

- The framework performs the same as it does for the event-driven application scenario and performs better than the online algorithm in the total values accrued and the number of payloads scheduled.
- Over the evaluation periods, the ratios move away from one. This is due to the unavailability of capacity to serve periods arriving later in the evaluation period due to the initial collection of the low valued periodic payload. This depletes the capacity faster, with fewer increments to the total value accrued.

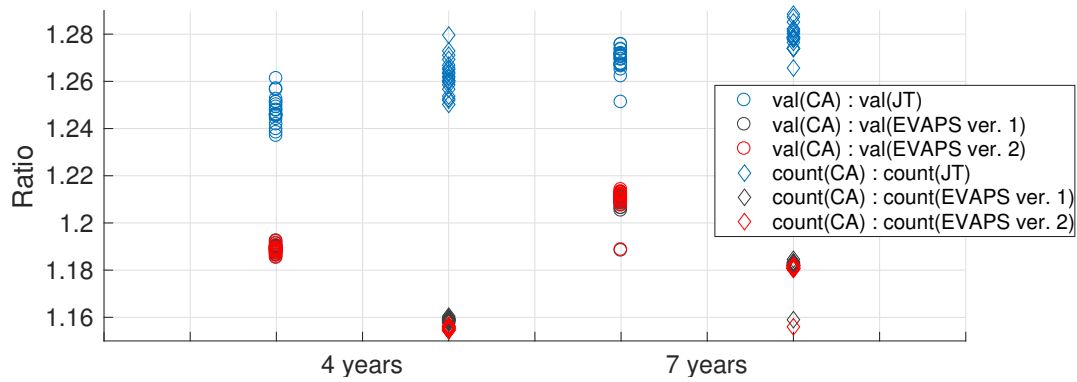


Figure 5.6: Periodic+events scenario: ratios of values accumulated, number of payloads scheduled by the clairvoyant algorithm to that of EVAPS ver. 1, EVAPS ver. 2 and Jumping threshold. The functions val() and count() returns the total value accumulated and the number of payloads scheduled.

5.2.3. CHAR EVALUATION

In the evaluation of the ChAR module in the xTEND framework, the NB-IoT device utilizes the 2 dB slack in the device transmission power [40], to reduce repetitions and extend lifetime. The experiments are carried out in coverage conditions where the repetitions allocated are greater than 2 (the RSRP value varies from -118 dB to -136 dB), the experimental setup is shown in Figure 5.7. The additional gain is varied in steps of 1 dB, and the number of repetitions is analyzed in each physical channel. The experiment comprises of performing a message transaction, with and without the additional gain. Each trial is repeated 22 times for both 1 dB and 2 dB additional gain transmissions. The energy consumption equations corresponding to transmission and reception, presented in Chapter 3, is used to estimate the energy savings for the physical channels - NPUSCH, NPDSCH, and NPDCCH - corresponding to each transport block. The energy consumption due to the cDRX time period, the idle mode, and the NPRACH are not included.

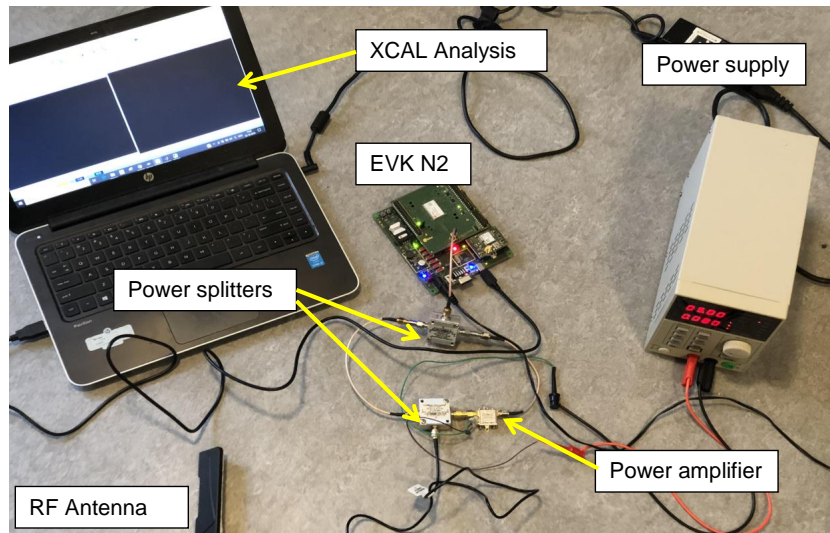


Figure 5.7: Experimental setup for ChAR evaluation

The combined energy savings in the NPUSCH, NPDSCH and NPDCCH channels are presented in the

Figure 5.8. With reduced repetitions, the time occupied in the NPDCCH, NPUSCH and NPDSCH channels is reduced. This has a direct impact on the scalability, as the devices finish the transactions faster. This is shown in Figure 5.9.

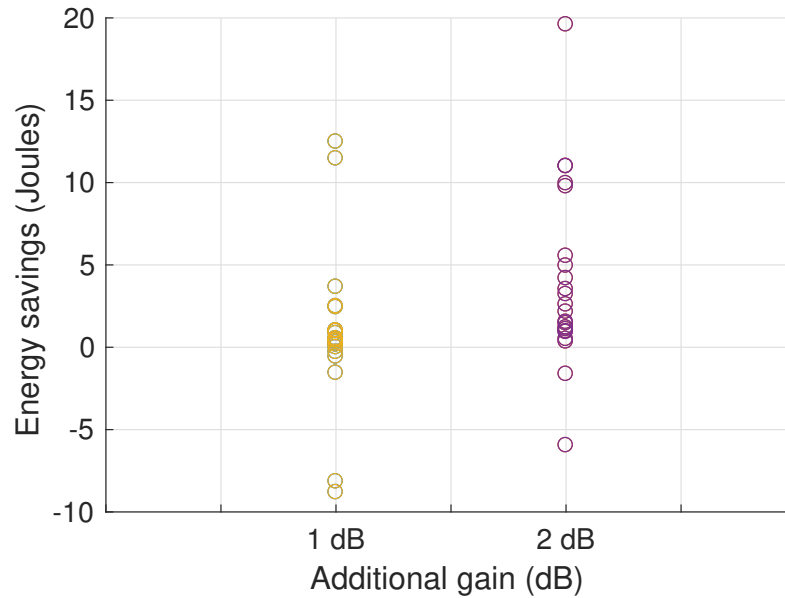


Figure 5.8: Energy savings with additional gain due to reduced coverage enhancement affects

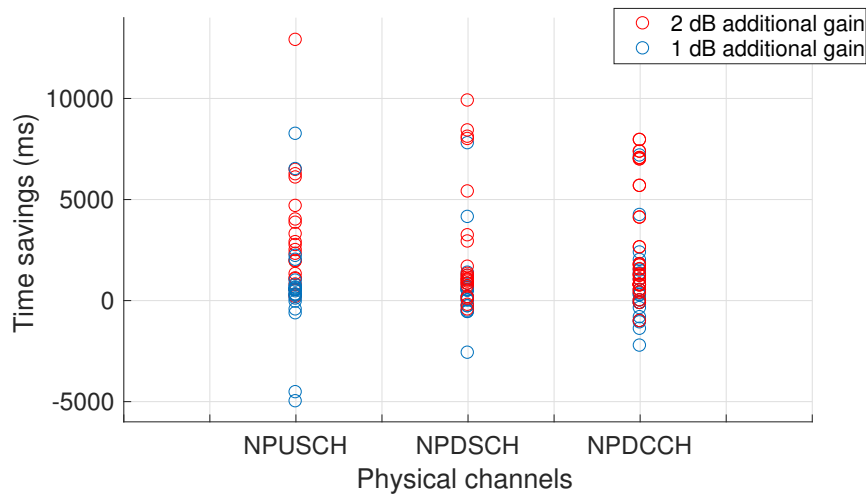


Figure 5.9: Time savings with additional gain due to reduced coverage enhancement affects

With the increased transmission power, the following was observed:

1. As expected, the repetition count of the transport blocks in both the uplink and the downlink reduces.
2. With the channel conditions, the device identifies the most suitable eNBs to attach. This implies that the reduction in repetitions is not always the same. They may vary depending on the link budget between the device and the eNB.

3. The device may perform cell-reselection and latch on to a new Physical Cell Id (PCI). Depending on the PCI the device connects to, timer configurations such as the inactivity timer differs. This has a direct impact on the lifetime of the device.
4. As a consequence of the reduction in energy by reducing repetitions, the duration of the device transactions (the duration the device is connected to the base station) reduces. However, the 'air-time' of the device (the duration for which device is connected to the base station) is also depended on parameters set at the eNB, such as the cDRX timer period, inactivity timer period etc.

Physical channel	Average time savings with 1 dB (ms)	Average time savings with 2 dB (ms)
NPUSCH	673.7143	3064
NPDSCH	669.4762	2596.318
NPDCCH	646.8095	2411.636

Table 5.1: Average time savings for each physical channel

Based on Figures 5.8 and 5.9, the following observations are made:

- On an average, the time savings obtained in each channel - NPUSCH, NPDSCH, and NPDCCH - with an additional gain of 2 dB is greater than that obtained with an additional gain of 1 dB. This is shown in Table 5.1.
- On an average, the energy savings with 2 dB additional gain (3.98 J) is greater than the energy savings with 1 dB additional gain (0.97 J). Hence, it benefits to utilize the entire slack of 2 dB.
- With the average energy savings of 3.98 J and combined time savings of 8.072 s, obtained with an additional gain of 2 dB, the device lifetime (without energy-harvesting) is extended by 22.48 % for bi-hourly reporting and 21.01 % for daily reporting in the deep coverage scenario.

5.3. SUMMARY

The xTEND framework constituting of the EVAPS module and the ChAR module is evaluated in this chapter. The EVAPS module is evaluated for the accumulated values of the messages and the number of payloads, for three distinct traffic distributions, serving messages of the same type (same weight, different values) and of a different type (different weight, different value). In all the cases, the EVAPS module was shown to perform better than the jumping threshold online algorithm. Further, the ChAR module was evaluated. The savings in energy and time are quantified for additional transmission power gain of 1 dB and 2 dB. The resulting impact in the lifetime of the device was calculated.

6

CONCLUSIONS AND FUTURE WORK

The work is concluded in this chapter, presenting the major discussion points and results. Further, proposals for future work is also presented.

6.1. CONCLUSIONS

This work characterizes the energy consumption of an NB-IoT device in real-world settings for various coverage scenarios. The energy consumption of an NB-IoT device for an end-to-end payload transactions is modeled. The lifetime of the device for various application scenarios, under different coverage conditions is estimated. The following are the observations made:

A device transmitting 200 bytes packet (including headers) and receiving a 65 bytes (including headers) packet lasts for 2.38 years and 77 days, for a daily and bi-hourly reporting interval, in deep coverage scenarios. This is significantly different from the expectations set in the 3GPP standards.

The major contributors to the low lifetime are the protocol (the signalling overheads, the timer configurations), the coverage enhancement techniques and the rate of message exchange as required by the application.

In order to increase the lifetime, the work investigates the possibility of harvesting energy from ambient sources. Three real-life data sets pertaining to ambient light in indoor and outdoor scenarios are analyzed. The gain obtained in terms of additional packets that can be served with the expected energy in all three scenarios is presented. It was found that in the best case that the device can operate perennially. However, this is highly dependent on the spatio-temporal profile of the energy sources. Therefore, the work presents the pressing challenges that need to be addressed in order to make the leap for a longer and sustainable NB-IoT solution.

To this end, we propose an energy extension framework that binds two schemes - Energy- and Value-Aware Packet Scheduler (EVAPS) and Channel Aware Radio block (ChAR)- to extend the lifetime of the NB-IoT device. The EVAPS module is formulated as a 0/1 incremental knapsack problem, with the energy buffer and the payloads forming the knapsack and the items for the knapsack, respectively. The ChAR block makes use of the 2 dBm tolerance in the maximum allowed transmission power. The

device identifies the channel conditions, and provides an additional gain in the transmission power if in deep coverage. The following summarizes the contributions/observations made:

An extension to the dynamic programming solution of solving the knapsack problem with incremental capacity, with the arrival of a single item at each time step is presented

A innovative threshold based scheme is presented, that forms capacity thresholds for each payload that guarantees the selection of the combination of payloads that form the maximum value in a given finite horizon.

The additional gain in transmission reduces the repetitions without losing coverage.

This results in reduction in energy spend by a device, and reduction in time a device occupies the physical channels - NPUSCH, NPDSCH, and NDCCH.

The xTEND framework is evaluated and performance analysis is performed. As the two modules operate independently, they are analyzed separately. The EVAPS module is evaluated for different traffic distributions (periodic, event-driven, periodic+event application). The total value and count of the payloads scheduled by the EVAPS module is compared with that of a jumping threshold online algorithm and the clairvoyant algorithm. The jumping threshold scheme has a competitive ratio of $(1 + \ln \frac{U}{L})$, where U and L represent the upper and lower bounds of the value-weight ratios of a payload. The ChAR module is evaluated with an additional gain step of 1 db. The experiments are carried out in deep coverage scenario. The following are the conclusions of the evaluation:

Given a set of value-weight ratios, the EVAPS module outperforms the online algorithm in all the three traffic distributions, given the flexibility to choose the finite horizon.

The average savings in energy and time obtained with a 2 dB additional gain is greater than that with a 1 dB additional gain.

With a 2 dB additional gain, the device on an average saves 3.8 J of energy and 8.072 sec in time. This results in a 20 %increase in the device lifetime in deep coverage scenarios.

Hence, by incorporating energy-harvesting technology with the xTEND framework, the research objective is met. The EVAPS module maximizes the utility of the device for the application, and the ChAR module counters the effects of the coverage enhancement techniques on the device lifetime.

6.2. FUTURE WORK

The problem of device lifetime is crucial for NB-IoT devices, and mandates solutions. The proposed xTEND framework can be implemented with the energy-harvesting technology to extend the time between depletions of the device battery, hence, extending device lifetime. The existing system can be enhanced with features that may be implemented in tandem with the existing features in the framework. Certain such aspects that would require further attention and form proposals for the future work are:

1. The threshold scheme proposed in this work is a fixed threshold scheme that can be easily tuned, based on the equation 4.6 presented in Chapter 4. The threshold scheme can be made adaptive with the changing channel conditions, by varying the finite horizon with the changing channel conditions. This involves identifying the ideal finite horizon for a given channel condition and updating the thresholds online. Implementing such a scheme would widen the scope of the framework to the dynamic channel scenarios extending to mobile application scenarios.

2. With energy prediction in a finite horizon, more payloads can be scheduled as the payloads that would otherwise be dropped due to lack of capacity would be scheduled. This benefits in applications where the payloads closer to the 'present' are more important than those in the 'future'. The threshold scheme can be extended to incorporate the additional incoming energy.
3. The ChAR module requires access to the power amplifier within the NB-IoT chipset. This requires further work in collaboration with the chipset vendors.
4. Other potential area of research is to investigate how to perform effective link adaptation by also considering the energy state of the device. This can effectively reduce the impact of the coverage enhancement techniques on the device lifetime.

PUBLICATIONS

1. Opportunitites and challenges for energy-harvesting in NB-IoT, (*to appear in ACM SigBed Review 2019*)
2. xTEND: Extending the Lifetime through Energy-harvesting for NarrowBand-IoT Developments (*submitted in IoTDI 2019*)

BIBLIOGRAPHY

- [1] link labs, *The past, present, future of lpwan*, (2018), [Accessed 23 Oct 2018].
- [2] RohdeSchwarz, *Narrowband internet of things whitepaper*, (2016).
- [3] O. Liberg, M. Sundberg, E. Wang, J. Bergman, and J. Sachs, *Cellular Internet of Things: Technologies, Standards, and Performance* (Academic Press, 2017).
- [4] ofinnotechs, *Internet of things*, (2018), [Accessed 23 Oct 2018].
- [5] Ericsson, *Cellular networks for massive iot*, (2016).
- [6] *Popular internet of things forecast of 50 billion devices by 2020 is outdated*, (2016), [Accessed 24 Mar 2018].
- [7] Huawei, *Nb-iot - enabling new business opportunities*, (2015).
- [8] 3GPP_TR45.820, *Cellular system support for ultra-low complexity and low throughput internet of things (ciot)(release 13)*, (2015).
- [9] K. Mekki, E. Bajic, F. Chaxel, and F. Meyer, *Overview of cellular lpwan technologies for iot deployment: Sigfox, lorawan, and nb-iot*, in *2nd International Workshop on Mobile and Pervasive Internet of Things, PerIoT 2018* (2018).
- [10] vodafone, *Narrowband-iot: pushing the boundaries of iot*, (2017).
- [11] S. Mumtaz, A. Alsohaily, Z. Pang, A. Rayes, K. F. Tsang, and J. Rodriguez, *Massive internet of things for industrial applications: Addressing wireless iot connectivity challenges and ecosystem fragmentation*, *IEEE Industrial Electronics Magazine* **11**, 28 (2017).
- [12] M. Lauridsen, H. Nguyen, B. Vejlggaard, I. Z. Kovács, P. Mogensen, and M. Sorensen, *Coverage comparison of gprs, nb-iot, lora, and sigfox in a 7800 km² area*, in *Vehicular Technology Conference (VTC Spring), 2017 IEEE 85th* (IEEE, 2017) pp. 1–5.
- [13] M. Lauridsen, R. Krigslund, M. Rohr, and G. Madueno, *An empirical nb-iot power consumption model for battery lifetime estimation*, in *Ieee Vts... Vehicular Technology Conference* (2018).
- [14] ublox, *Ublox sara n211 nb-iot module for europe; cat nb1*, (2018), [Accessed 31 Mar 2018].
- [15] M. Solutions, *Mobile device power monitor manual,ver 1.14*, (2014), [Accessed 03 Mar, 2018].
- [16] M. Shirvanimoghaddam, K. Shirvanimoghaddam, M. M. Abolhasani, M. Farhangi, V. Z. Barsari, H. Liu, M. Dohler, and M. Naebe, *Paving the path to a green and self-powered internet of things*, arXiv preprint arXiv:1712.02277 (2017).
- [17] P. Andres-Maldonado, P. Ameigeiras, J. Prados-Garzon, J. Navarro-Ortiz, and J. M. Lopez-Soler, *Narrowband iot data transmission procedures for massive machine-type communications*, *IEEE Network* **31**, 8 (2017).
- [18] B. Martinez, F. Adelantado, A. Bartoli, and X. Vilajosana, *Exploring the performance boundaries of nb-iot*, arXiv preprint arXiv:1810.00847 (2018).

- [19] M. E. Soussi, P. Zand, F. Pasveer, and G. Dolmans, *Evaluating the performance of emtc and nb-iot for smart city applications*, arXiv preprint arXiv:1711.07268 (2017).
- [20] R. Ratasuk, B. Vejlgaard, N. Mangalvedhe, and A. Ghosh, *Nb-iot system for m2m communication*, in *Wireless Communications and Networking Conference (WCNC), 2016 IEEE* (IEEE, 2016) pp. 1–5.
- [21] H. Kroll, M. Korb, B. Weber, S. Willi, and Q. Huang, *Maximum-likelihood detection for energy-efficient timing acquisition in nb-iot*, in *Wireless Communications and Networking Conference Workshops (WCNCW), 2017 IEEE* (IEEE, 2017) pp. 1–5.
- [22] C. Yu, L. Yu, Y. Wu, Y. He, and Q. Lu, *Uplink scheduling and link adaptation for narrowband internet of things systems*, *IEEE Access* **5**, 1724 (2017).
- [23] Q. Mu, L. Liu, H. Jiang, K. Takeda, and R. Ma, *Investigation on link adaptation for lte-based machine type communication*, in *Vehicular Technology Conference (VTC Spring), 2016 IEEE 83rd* (IEEE, 2016) pp. 1–5.
- [24] S. Xu, Y. Liu, and W. Zhang, *Grouping-based discontinuous reception for massive narrowband internet of things systems*, *IEEE Internet of Things Journal* **5**, 1561 (2018).
- [25] A. S. Weddell, M. Magno, G. V. Merrett, D. Brunelli, B. M. Al-Hashimi, and L. Benini, *A survey of multi-source energy harvesting systems*, in *Proceedings of the conference on design, automation and test in Europe* (EDA Consortium, 2013) pp. 905–908.
- [26] R. V. Prasad, S. Devasenapathy, V. S. Rao, and J. Vazifehdan, *Reincarnation in the ambiance: Devices and networks with energy harvesting*, *IEEE Communications Surveys & Tutorials* **16**, 195 (2014).
- [27] C. Moser, L. Thiele, D. Brunelli, and L. Benini, *Adaptive power management for environmentally powered systems*, *IEEE Transactions on Computers* **59**, 478 (2010).
- [28] C. M. Vigorito, D. Ganesan, and A. G. Barto, *Adaptive Control Wireless Sensor Networks*, *IEEE International Conference on Sensing, Communication and Networking*, 21 (2007).
- [29] A. Kansal, J. Hsu, S. Zahedi, and M. B. Srivastava, *Power management in energy harvesting sensor networks*, *ACM Transactions on Embedded Computing Systems (TECS)* **6**, 32 (2007).
- [30] M. A. Alsheikh, D. T. Hoang, D. Niyato, H.-P. Tan, and S. Lin, *Markov decision processes with applications in wireless sensor networks: A survey*, arXiv preprint arXiv:1501.00644 (2015).
- [31] J. Lei, R. Yates, and L. Greenstein, *A generic model for optimizing single-hop transmission policy of replenishable sensors*, *IEEE Transactions on Wireless Communications* **8**, 547 (2009).
- [32] S. Mao, M. H. Cheung, and V. W. Wong, *An optimal energy allocation algorithm for energy harvesting wireless sensor networks*, in *Communications (ICC), 2012 IEEE International Conference on* (IEEE, 2012) pp. 265–270.
- [33] N. Michelusi, K. Stamatiou, and M. Zorzi, *Transmission policies for energy harvesting sensors with time-correlated energy supply*, *IEEE Transactions on Communications* **61**, 2988 (2013).
- [34] D. Bienstock, J. Sethuraman, and C. Ye, *Approximation algorithms for the incremental knapsack problem via disjunctive programming*, arXiv preprint arXiv:1311.4563 (2013).
- [35] E. T. Ceran, T. Erkilic, E. Uysal-Biyikoglu, T. Girici, and K. Leblebicioglu, *Optimal energy allocation policies for a high altitude flying wireless access point*, *Transactions on Emerging Telecommunications Technologies* **28**, e3034 (2017).

-
- [36] M. Gorlatova, M. Zapas, E. Xu, M. Bahlke, I. J. Kymissis, and G. Zussman, *CRAW-DAD dataset columbia/enhants (v. 2011-04-07)*, Downloaded from <https://crawdad.org/columbia/enhants/20110407> (2011).
- [37] KNMI, *Knmi - uurgegevens van het weer in nederland - download*, (2018).
- [38] 3GPP_TS36.213, *evolved universal terrestrial radio access (e-utra) - physical layer procedures*, (2018).
- [39] P. Toth, *Dynamic programming algorithms for the zero-one knapsack problem*, *Computing* **25**, 29 (1980).
- [40] ETSI, *Lte; evolved universal terrestrial radio access (e-utra); user equipment (ue) radio transmission and reception (3gpp ts 36.101 version 13.4.0 release 13)*, (2016).
- [41] *Patras: Internet of things case study*, (2017).
- [42] *China mobile smart parking – internet of things case study*, (2018).
- [43] *Uspace smart parking internet of things case study*, (2018).
- [44] smart parking systems, *First smart parking installation in spain with nb-iot sensors*, (2018), [Accessed 23 Oct 2018].